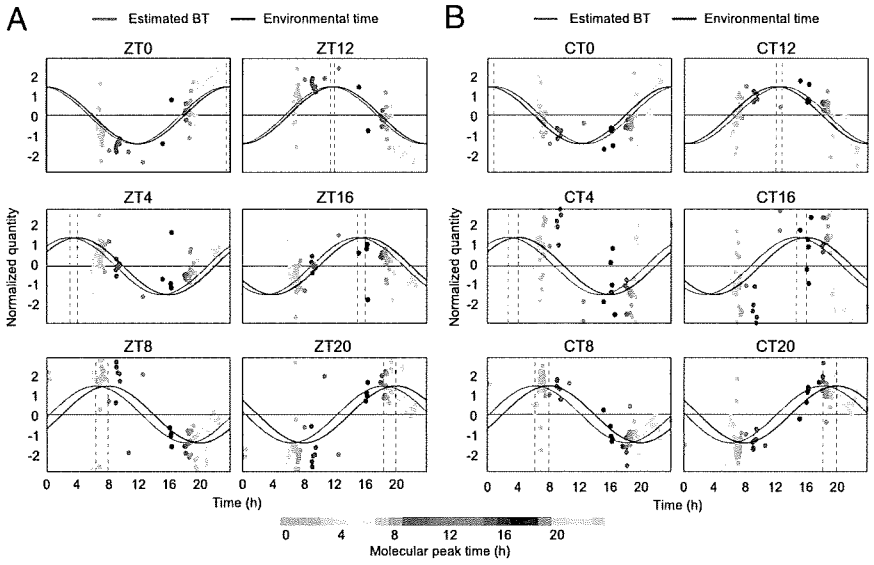

Fig. 2. BT estimation. BT measurements of mice kept under LD (*A*) and DD (*B*) conditions. Colors of the dots indicate the molecular peak times of each substance (Table S1). Peak time of the red cosine curves indicates estimated BT and peak time of the blue indicates the time the sample was taken ("environmental time"). The greater the degree of overlap of the red and blue curves, the greater the accuracy of the measurement. The dashed vertical lines show the BT (red) or environmental time (ZT/CT, blue). See Table S2 for statistics.

tion errors of 1.0 ± 0.49 h for LD and 1.3 ± 0.45 h for DD (mean ± SD, Table S2). Estimation error was here defined as time difference between estimated BT and sampling time (environmental time). These results suggest that BT can be accurately determined from the metabolite profiles of independently sampled mice.

Differences in Genetic Backgrounds. In clinical situations, methods for BT detection must apply to populations with heterogeneous genetic backgrounds. To demonstrate the suitability of the metabolite-timetable method for individuals with different genetic backgrounds, we applied the method to other inbred mouse strain with genetic backgrounds that differed from the original CBA/N strain. We chose C57BL/6, because C57BL/6 and CBA/N are genetically remote from each other and classified into 2 completely different clusters among 55 mice strains according to SNP-based study (38). We collected the blood plasma samples from individual young male C57BL/6 mice every 4 h over 24 h under LD and DD conditions and quantified the time-indicating metabolites in the plasma by LC-MS (Fig. 3 *A* and *B*). The metabolite-timetable method detected significant circadian rhythmicity ($P < 0.01$) in all metabolite profiles both under LD (Fig. 3*A*) and DD conditions (Fig. 3*B*) even if we used the metabolite timetable constructed from CBA/N mice. The estimated BT closely matched with the environmental time with the estimation errors of 1.6 ± 0.36 h for LD and 1.7 ± 0.24 h for DD (mean ± SD, Table S2). These results suggest that BT can be accurately determined from the metabolite profiles of mice with heterogeneous genetic backgrounds.

Differences in Age and Sex. We constructed the metabolite timetable from young male mice only, so it was possible that age and sex factors might affect the accuracy of the metabolite-timetable method. To determine the influence of age and sex, we also applied the metabolite-timetable method to aged male and young female mice of the same strain. Blood plasma from individual aged male or young female CBA/N mice was sampled at 2 time points, ZT0 (the beginning of the day, i.e., time of light on) and ZT12 (the end of the day, i.e., time of the light off) under LD condition. These time points were considered as 2 "noisiest" time points, because light conditions were dramatically changed at these points. Time-indicating metabolites in the plasma were quantified by LC-MS (Fig. 4*A*) and significant circadian rhythmicity ($P < 0.01$) was detected in all metabolite profiles of both the aged male mice and

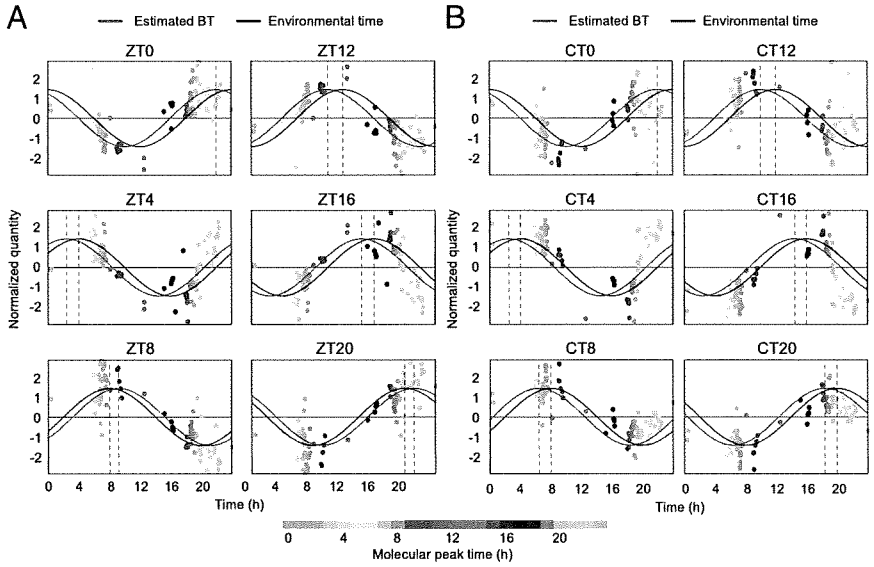

Fig. 3. Genetic background. BT measurement using C57BL/6 mice plasma collected under LD (*A*) and DD (*B*) conditions. Colors of the dots indicate the molecular peak times of each substance (Table S1). Peak time of the red cosine curves indicate estimated BT and peak time of the blue indicate the environmental time. The dashed vertical lines show the BT (red) or environmental time (ZT/CT, blue). See Table S2 for statistics.

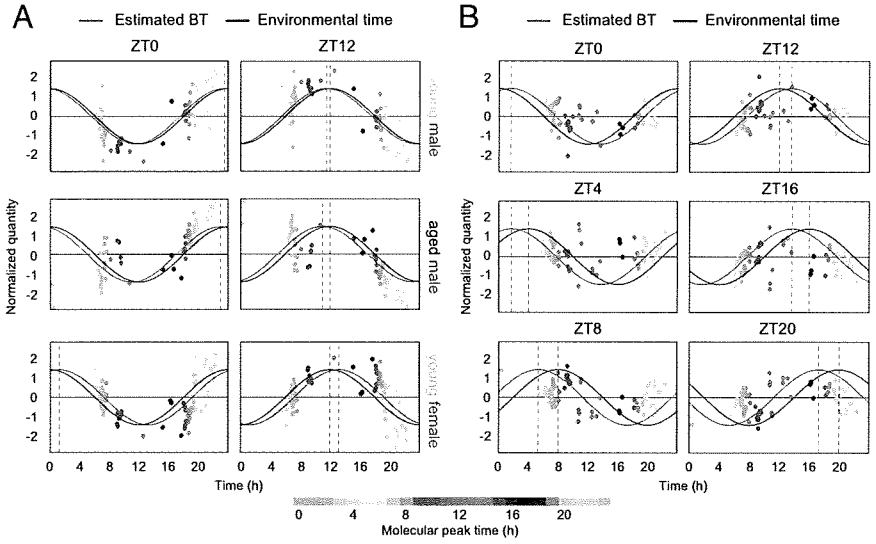

Fig. 4. Age, sex differences and feeding condition. (*A*) BT measurement of young male (*Top*), aged male (*Middle*), and young female mice plasma (*Bottom*) harvested at ZT0 (*Left*) and ZT12 (*Right*). (*B*) BT measurement of young male mice kept under food-deprivation conditions. Colors of the dots indicate the molecular peak times of each substance (Table S1). Peak time of the red cosine curves indicates estimated BT, and peak time of the blue indicates the environmental time. The dashed vertical lines show the BT (red) or environmental time (ZT, blue). Results for young male mice (*A*) are replotted from Fig. 2*A* for comparison. See also Table S2 for statistics.

the young female CBA/N mice (Fig. 4*A*). The estimated BT from individual mice sampled at ZT0 and ZT12 were BT23.0 and BT11.0 in aged male mice and BT1.2 and BT13.2 in young female mice (Table S2). These results demonstrate that BT can be accurately determined from the metabolite profiles of mice of different age and sex.

Differences in Feeding Conditions. The circadian rhythmicity of food intake is well known (39); therefore, feeding conditions may severely affect the accuracy of the metabolite-timetable method. To validate the use of the metabolite timetable in individuals with different feeding conditions, we applied the metabolite-timetable method to CBA/N mice deprived of food (food deprivation). This feeding condition differed greatly from the original feeding condition where CBA/N mice were allowed ad lib feeding. We collected the blood plasma from individual young, male, food-deprived CBA/N mice every 4 hours over 24 h under LD condition. LC-MS analysis was performed to quantify the plasma metabolites (Fig. 4*B*). The metabolite-timetable method detected significant circadian rhythmicity ($P < 0.03$) in all metabolite profiles. The estimated BT matched with the environmental time with the estimation errors of 2.2 ± 0.50 h (mean ± SD, Table S2). These results suggest that BT can be determined from the metabolite profiles of mice even under severe feeding conditions.

Detection of Jet Lag. The final stage of the study was to evaluate the use of the metabolite-timetable in the diagnosis of circadian rhythm disorders. Jet lag is a common disorder of circadian rhythm, in which there is a difference between the internal BT and environmental time. To mimic jet lag, we kept the mice for 2 weeks under normal LD conditions and then rapidly advanced the lighting schedule by 8 h (40). Plasma samples were analyzed at 2 time points (ZT0 and ZT12 of the original LD cycle, termed as "Time 1" and "Time 2") on 3 separate days: on day 1 (before entrainment to the new cycle), day 5 (during entrainment), and day 14 (after entrainment) (Fig. 5 *A* and *B*). On day 1, the estimated BTs were 23.8 h (Time 1) and 11.8 h (Time 2), suggesting that the internal BTs still follow the original LD cycle. By day 14, estimated BTs were 8.8 h (Time 1) and 20.8 h (Time 2), suggesting that the internal BTs had shifted by ≈8 h from the original LD cycle and had therefore become entrained completely to the advanced cycle. Notably, on day 5, estimated BTs were 3.5 h (Time 1) and 15.5 h (Time 2), a shift

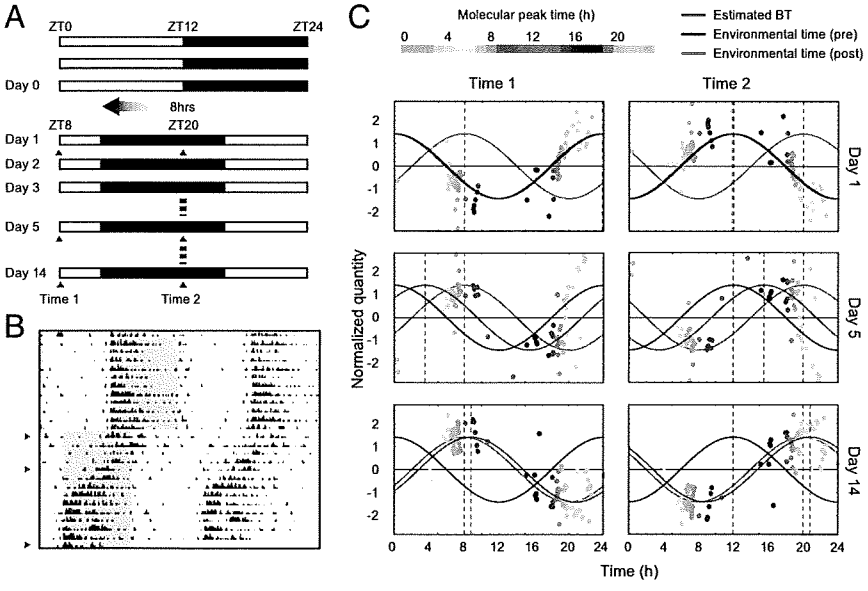

Fig. 5. Detection of jet lag. (*A*) Schematic view of lighting conditions. White bars indicate light on, and black bars indicate light off. On day 1, the light was turned off 8 h earlier. Samples were collected at 2 time points on days 1, 5, and 14 after the LD shift (red triangles). (*B*) The actogram of a single mouse, showing that it was experiencing "jet lag" induced by the LD shift. Yellow shading indicates periods of light on, and gray shading indicates periods of light off. The red triangles indicate days 1 (*Top*), 5 (*Middle*), and 14 (*Bottom*). (*C*) BT measurement from mouse plasma collected before (day 1, *Top*), during (day 5, *Middle*), and after entrainment to the new LD cycle (day 14, *Lower*). Colors of the dots indicate the molecular peak time of each substance (Table S1). The red cosine curve is the estimation, the blue curve is the environmental time (pre LD condition shift), and the brown cosine curve is the environmental time (post shift). See also Table S2 for statistics.

of 3.5 h from the original LD cycle, indicating incomplete entrainment to the advanced cycle, i.e., jet lag (Fig. 5*C* and Table S2). These results suggest that the metabolite-timetable method can accurately detect circadian rhythm disorders. Another set of BT estimation data for jet-lagged mice supports this conclusion (Fig. S2 and Table S2).

General Applicability of the Metabolite-Timetable Method: CE-MS-Based Method. As described above, the metabolite-timetable method based on LC-MS analysis can accurately measure the individual's BT and sensitively diagnose circadian rhythm disorders such as jet lag. The method depends entirely on the oscillations of numerous chemical substances and time-indicating metabolites; therefore, it can be applied to other metabolomics technologies such as CE-MS analysis. With CE-MS analysis, it is possible to separate charged compounds. So this is a complementary technology to LC-MS analysis (35). To demonstrate the general applicability of the metabolite-timetable method to other metabolomics technology, blood plasma was sampled and pooled from young male CBA/N mice every 4 hours under LD or DD conditions over 2 days. Small positively charged chemical substances in these samples were quantified by CE-MS, which detected 953 peaks. Of these peaks, 153 exhibited significant circadian oscillations under LD and DD conditions (Fig. S3*A*). We used these CE-MS data to construct the metabolite timetable in mouse plasma (Table S3). Notably, 28 peaks (18.3% of the total) were identified as known metabolites (Fig. S3*B*).

To confirm whether the CE-MS-based metabolite timetable was a good indicator of an individual's BT, we estimated BT from the metabolite profiles of independently sampled mice. Fresh plasma from young male CBA/N mice was collected every 4 hours over 24 h both under LD and DD conditions. CE-MS analysis was performed to profile the time-indicating metabolites (Fig. S3 *C* and *D*). The CE-MS-based metabolite-timetable method detected significant circadian rhythmicity in all metabolite profiles of these samples ($P < 0.01$, Fig. S3 *C* and *D*). The estimated BT was close to the environmental time with estimation errors of 0.6 ± 0.29 h for LD and 0.6 ± 0.54 h for DD (mean ± SD, Table S4). These results suggest the metabolite-timetable method is generally applicable to other metabolomics technologies such as CE-MS. See Fig. S3 *E–H* and *SI Text* for the result at a more stringent criterion (FDR < 0.01).

Discussion

We identified 14 and 28 oscillatory peaks in mouse blood as known metabolites in LC-MS and CE-MS analysis, respectively. For example, a different type of lysophsophatidylcolines exhibit significant circadian oscillations in LC-MS analysis (Fig. 1 *C* and *D*). The genes for key enzymes synthesizing lysophosphatidylcoline are *Lcat* (lecitine:cholesterol acyltransferase), *Lipc* (hepatic lipase), and *Lipg* (endothelial lipase). Among these genes, *Lcat* and *Lipc* are mainly expressed in liver. We found that *Lipc* mRNA are rhythmically expressed in the mouse liver with the peak time around peak time (PT) 5 (8), which slightly proceeds with the peak time of identified oscillatory lysophosphatidylcolines (PT5.8–9.1). In CE-MS analysis, many amino acids exhibit significant circadian rhythmicity. For example, glutamine (Gln), threonine (Thr), proline (Pro), valine (Val), phenylalanine (Phe), methionine (Met), isoleucine (Ile), leucine (Leu), and tryptophan (Trp) peak at around midnight (≈PT18), whereas glycine (Gly) peaks in the evening (PT12.1) (Fig. S4). In the urea cycle, metabolites such as ornithine (PT18.6), citrulline (PT19.9), and 4-guanidino-butyrate (PT20.1) exhibit significant circadian rhythmicity (FDR <0.1). Arginine (Arg), which plays an important role in the urea cycle, also exhibits suggestive circadian rhythmicity (FDR = 0.215; PT0.6) in our CE-MS data. It is also noteworthy that the final product—Urea—is reported to vary over 24 h in the blood of certain species such as rabbits (41) and rats (42). Interestingly, Reddy et al. (43) showed that 3 key enzymes involved in the urea cycle, carbamoyl-phosphate synthetase 1 (CPS1), argininosuccinate synthetase 1 (ASS1), and arginase 1 (ARG1), show circadian rhythms in the liver, the center of the urea cycle and urea formation (43). In the creatine pathway and neighboring glycine and threonine metabolism, metabolites such as guanidoacetate (PT6.2), Creatine (PT14.7), creatinine (PT18.7), sarcosine (PT18.0), and dimethylglycine (PT16.5) exhibit significant circadian rhythmicity (FDR <0.1). Arginine (PT0.6) first converts to guanidoacetate. Guanidoacetatete (CT6.2) then converts to creatine. Creatine (PT14.7) finally converts to creatinine (PT18.7) or sarcosine (PT18.0), which is also converted from dimethylglycine (PT16.5). The differences in the peak times of these metabolites may reflect successive processing throughout the day in the creatine pathway and neighboring glycine and threonine metabolism (Fig. S4).

Our results suggest that metabolite-timetable method can detect circadian rhythm disorders in vivo. In a normal situation, patients live under the zeitgeber (e.g., light). Notably, our method successfully diagnoses the jet-lag state under LD conditions (Fig. 5 and Fig. S2), and this strongly suggests that endogenous abnormal clock state can be diagnosed by our method, even if there is external time information such as light. Circadian rhythm disorders are caused by environmental factors (such as jet lag) and/or inherited factors (as in familial advanced sleep-phase syndrome). Brown et al. (44, 45) reported detecting circadian rhythm disorders by characterizing the feature of molecular circadian clocks in the isolated cells. They collected skin samples from human subjects, cultured the cells, and transfected clock-controlled reporter into the cells. The features of the molecular circadian clock in the isolated cells correlated with the chronotypes (i.e., the feature of organismal circadian clock) of the subjects, suggesting that the method should also allow detection of inherited circadian rhythm disorders. Our method can detect both inherited and acquired circadian rhythm disorders but cannot distinguish between them, whereas Brown et al.'s (44, 45) method can detect inherited but not acquired disorders. These 2 methods are therefore complementary for detecting circadian rhythm disorders.

Although our results suggest the metabolite-timetable method can successfully estimate BT, keeping MS and hiring a specialized operator in each hospital seems difficult. Establishing a special center for "detecting BT" performing MS analysis is 1 possibility to solve this. Another possibility is detecting time-indicating metabolites in a specific way (e.g., making an ELISA kit for detecting BT using a specific antibody for target time-indicating metabolites). To achieve the latter possibility, the assignment of oscillatory peaks to known metabolites is important, and we already identified 14 (LC-MS) and 28 (CE-MS) oscillatory peaks as known metabolites (Figs. 1 and S3). We also examined the effect of peak numbers on BT estimation. Fig. S5 shows the accuracy of the BT estimation using the different number of oscillatory metabolites. If we set the statistical error rate $P < 0.05$ and estimation error between environmental and estimated time <2 h, the minimum number of time-indicating metabolites was ≈20. In addition, the effect of feeding is an important issue, especially in humans, because humans eat different amounts of food at entirely different times. Further analysis on food intake conditions would be a great help for applying this method in clinical situations.

In this study, we showed that a metabolite-timetable method based on LC–MS analysis is able to estimate individuals' BTs with a high degree of accuracy throughout the time of the day, under different lighting conditions (LD and DD), and in individuals with different genetic backgrounds (CBA/N and C57BL/6 mice) (Figs. 2 and 3). We also found that the LC–MS-derived metabolite timetable is robust despite differences in age, sex, and feeding (Fig. 4); in addition, it is a sensitive and accurate detector of disordered circadian rhythm in jet-lagged mice. Our preliminary results suggest that the metabolite-timetable method can be also applied to other metabolomics techniques such as CE–MS; it allowed quantification of hundreds of clock-controlled metabolites, of which many could

be identified, enabling successful measurement of BT from independent blood samples. The next step is to construct a metabolite timetable for human blood plasma, which will help measurement of BTs for humans and diagnosis of circadian rhythm disorders and facilitate the development of chronotherapy and tailored medication regimens.

Materials and Methods

BT Measurement. Metabolomics-based measurement of BT is performed as described for expression-based measurement of BT (16), except that 2 samples are used for an estimation of BT. In the metabolite-timetable method, we used 2 samples with 12-h sampling time interval (e.g., ZT0 and ZT12 are used for 1 measurement of BT) to calibrate measurement-to-measurement experimental fluctuations of detection sensitivity, which usually differs among metabolites. We define the area in a certain sample as A_{si} and the mean areas of 2 samples (of 12-h time interval) as M_{si} for metabolite i. We also define the mean, standard deviation, and peak time of metabolite i in the timetable as M_{ti}, S_{ti}, and p_{ti}, respectively. For estimation of BT, we did not use outlying metabolites that do not satisfy the condition $(|(M_{ti} - M_{si})/S_{ti}| < 2\sqrt{2})$. By changing b to 0, 0.1, . . . , 23.9, we searched for b with a maximum Pearson's correlation between $\{\sqrt{2}\cos(2\pi(P_{ti} - b)/24)\}$ and $\{(A_{si} - M_{si})/S_{ti}\}$, and we predicted b as BT of the target sample. To estimate the P value of the prediction, we applied a permutation test to the maximum correlations.

Ethics. All experiments were performed with the permission of Kobe Animal Experiment Supervisory Panel (permission IDs are AH15-10 and AH18-01).

Supporting Information. More Materials and Methods information is available in *SI Text*.

ACKNOWLEDGMENTS. We thank Sachie Satoh and Yuki Ueno for technical support. We also thank Shigenobu Shibata, Masamitsu Iino, Kenichiro Uno, Rikuhiro Yamada, Hideki Ukai, Guojun Sheng, Yasushi Isojima, and Sato Honma for helpful discussions and Erik Kuld for proofreading of the manuscript. The Laboratory for Animal Resources and Genetic Engineering in the Center for Developmental Biology is noted for assistance with mouse work. This work is partly supported by New Energy Developing Organization (NEDO) (H.R.U.), a grant on Priority Aeas "Ensuring Chemical Hazard" and "Biomarker Discovery for Drug Development" from the Health and Labor Sciences Research Grants (T.S.), and a grant "Functional Genomics on Fundamental Brain Functions" from Utsunomiya University (M.I.).

1. Dunlap JC, Loros JJ, DeCoursey PJ, eds (2004) *Chronobiology: Biological Timekeeping* (Sinauer, Sunderland, MS).
2. Reppert SM, Weaver DR (2002) Coordination of circadian timing in mammals. *Nature* 418:935–941.
3. Ueda HR (2007) Systems biology of mammalian circadian clocks. *Cold Spring Harb Symp Quant Biol* 72:365–380.
4. Takahashi JS, Hong HK, Ko CH, McDearmon EL (2008) The genetics of mammalian circadian order and disorder: Implications for physiology and disease. *Nat Rev Genet* 9:764–775.
5. Akhtar RA, et al. (2002) Circadian cycling of the mouse liver transcriptome, as revealed by cdna microarray, is driven by the suprachiasmatic nucleus. *Curr Biol* 12:540–550.
6. Panda S, et al. (2002) Coordinated transcription of key pathways in the mouse by the circadian clock. *Cell* 109:307–320.
7. Storch KF, et al. (2002) Extensive and divergent circadian gene expression in liver and heart. *Nature* 417:78–83.
8. Ueda HR, et al. (2002) A transcription factor response element for gene expression during circadian night. *Nature* 418:534–539.
9. Halberg F (1969) Chronobiology. *Annu Rev Physiol* 31:675–725.
10. Labrecque G, Belanger PM (1991) Biological rhythms in the absorption, distribution, metabolism and excretion of drugs. *Pharmacol Ther* 52:95–107.
11. Lemmer B, Scheidel B, Behne S (1991) Chronopharmacokinetics and chronopharmacodynamics of cardiovascular active drugs. Propranolol, organic nitrates, nifedipine. *Ann NY Acad Sci* 618:166–181.
12. Reinberg A, Halberg F (1971) Circadian chronopharmacology. *Annu Rev Pharmacol* 11:455–492.
13. Reinberg A, Smolensky M, Levi F (1983) Aspects of clinical chronopharmacology. *Cephalalgia 3 Suppl* 1:69–78.
14. Levi F, Zidani R, Misset JL (1997) Randomised multicentre trial of chronotherapy with oxaliplatin, fluorouracil, and folinic acid in metastatic colorectal cancer. International organization for cancer chronotherapy. *Lancet* 350:681–686.
15. Ohdo S, Koyanagi S, Suyama H, Higuchi S, Aramaki H (2001) Changing the dosing schedule minimizes the disruptive effects of interferon on clock function. *Nat Med* 7:356–360.
16. Ueda HR, et al. (2004) Molecular-timetable methods for detection of body time and rhythm disorders from single-time-point genome-wide expression profiles. *Proc Natl Acad Sci USA* 101:11227–11232.
17. Kennaway DJ, Owens JA, Voultsios A, Varcoe TJ (2006) Functional central rhythmicity and light entrainment, but not liver and muscle rhythmicity, are clock independent. *Am J Physiol* 291:R1172–R1180.
18. Kennaway DJ, Voultsios A, Varcoe TJ, Moyer RW (2002) Melatonin in mice: Rhythms, response to light, adrenergic stimulation, and metabolism. *Am J Physiol* 282:R358–R365.
19. Takahashi Y, Kipnis DM, Daughaday WH (1968) Growth hormone secretion during sleep. *J Clin Invest* 47:2079–2090.
20. Schoeller DA, Cella LK, Sinha MK, Caro JF (1997) Entrainment of the diurnal rhythm of plasma leptin to meal timing. *J Clin Invest* 100:1882–1887.
21. Kok P, et al. (2006) Increased circadian prolactin release is blunted after body weight loss in obese premenopausal women. *Am J Physiol* 290:E218–E224.
22. Breum L, Rasmussen MH, Hilsted J, Fernstrom JD (2003) Twenty-four-hour plasma tryptophan concentrations and ratios are below normal in obese subjects and are not normalized by substantial weight reduction. *Am J Clin Nutr* 77:1112–1118.
23. Forslund AH, et al. (2000) Inverse relationship between protein intake and plasma free amino acids in healthy men at physical exercise. *Am J Physiol Endocrinol Metab* 278:E857–E867.
24. Blanco RA, et al. (2007) Diurnal variation in glutathione and cysteine redox states in human plasma. *Am J Clin Nutr* 86:1016–1023.
25. Bonsch D, et al. (2007) Daily variations of homocysteine concentration may influence methylation of DNA in normal healthy individuals. *Chronobiol Int* 24:315–326.
26. Fernie AR, Trethewey RN, Krotzky AJ, Willmitzer L (2004) Metabolite profiling: From diagnostics to systems biology. *Nat Rev Mol Cell Biol* 5:763–769.
27. Kell DB, et al. (2005) Metabolic footprinting and systems biology: The medium is the message. *Nat Rev Microbiol* 3:557–565.
28. Villas-Boas SG, Mas S, Akesson M, Smedsgaard J, Nielsen J (2005) Mass spectrometry in metabolome analysis. *Mass Spectrom Rev* 24:613–646.
29. Fiehn O, et al. (2000) Metabolite profiling for plant functional genomics. *Nat Biotechnol* 18:1157–1161.
30. Fiehn O, Kopka J, Trethewey RN, Willmitzer L (2000) Identification of uncommon plant metabolites based on calculation of elemental compositions using gas chromatography and quadrupole mass spectrometry. *Anal Chem* 72:3573–3580.
31. Schauer N, et al. (2006) Comprehensive metabolic profiling and phenotyping of interspecific introgression lines for tomato improvement. *Nat Biotechnol* 24:447–454.
32. Plumb R, et al. (2003) Metabonomic analysis of mouse urine by liquid-chromatography-time of flight mass spectrometry (lc-tofms): Detection of strain, diurnal and gender differences. *Analyst* 128:819–823.
33. Wilson ID, et al. (2005) High resolution "Ultra performance" Liquid chromatography coupled to oa-tof mass spectrometry as a tool for differential metabolic pathway profiling in functional genomic studies. *J Proteome Res* 4:591–598.
34. Tolstikov VV, Lommen A, Nakanishi K, Tanaka N, Fiehn O (2003) Monolithic silica-based capillary reversed-phase liquid chromatography/electrospray mass spectrometry for plant metabolomics. *Anal Chem* 75:6737–6740.
35. Soga T, et al. (2006) Differential metabolomics reveals ophthalmic acid as an oxidative stress biomarker indicating hepatic glutathione consumption. *J Biol Chem* 281:16768–16776.
36. Soga T, et al. (2003) Quantitative metabolome analysis using capillary electrophoresis mass spectrometry. *J Proteome Res* 2:488–494.
37. van der Horst GT, et al. (1999) Mammalian cry1 and cry2 are essential for maintenance of circadian rhythms. *Nature* 398:627–630.
38. Tsang S, et al. (2005) A comprehensive snp-based genetic analysis of inbred mouse strains. *Mamm Genome* 16:476–480.
39. Froy O, Miskin R (2007) The interrelations among feeding, circadian rhythms and ageing. *Prog Neurobiol* 82:142–150.
40. Moriya T, et al. (1998) Potentiating action of mkc-242, a selective 5-ht1a receptor agonist, on the photic entrainment of the circadian activity rhythm in hamsters. *Br J Pharmacol* 125:1281–1287.
41. Piccione G, Caola G, Refinetti R (2007) Daily rhythms of liver-function indicators in rabbits. *J Physiol Sci* 57:101–105.
42. Kato H, Mizutani-Funahashi M, Shiosaka S, Nakagawa H (1978) Circadian rhythms of urea formation and argininosuccinate synthetase activity in rat liver. *J Nutr* 108:1071–1077.
43. Reddy AB, et al. (2006) Circadian orchestration of the hepatic proteome. *Curr Biol* 16:1107–1115.
44. Brown SA, et al. (2005) The period length of fibroblast circadian gene expression varies widely among human individuals. *PLoS Biol* 3:e338.
45. Brown SA, et al. (2008) Molecular insights into human daily behavior. *Proc Natl Acad Sci USA* 105:1602–1607.

FULL PAPER *Physiology*

Androgen Suppresses Corticotropin-Induced Increase in Plasma Cortisol Level but Enhances The Increase in Plasma Aldosterone Level in Goats

Masato AOYAMA[1)]*, Yuko MAEJIMA[1)]**, Toshio SUZUKI[1)], Masayuki IIGO[2)] and Shoei SUGITA[1)]

[1)]*Departments of Animal Science and* [2)]*Applied Biochemical Science, Faculty of Agriculture, Utsunomiya University, 350 Minemachi, Utsunomiya-Shi, 321–8505, Japan*

(Received 14 August 2008/Accepted 1 November 2008)

ABSTRACT. Previously we reported that androgen treatment reduced the extent of the increase in plasma cortisol (Cor) levels induced by adrenocorticotropic hormone (ACTH) administration in goats. In this study, we investigated the effect of androgen on the plasma levels of androstenedione and aldosterone. Four castrated male goats, which were treated with either 5α-dihydrotestosterone (DHT) or cholesterol (cho), were injected intravenously with 0.005, 0.02 or 0.1 mg of ACTH(1–24). Plasma Cor levels were increased significantly by all doses of ACTH injection, and these extents were lower in DHT-treated goats. Plasma androstenedione levels were also increased by ACTH injection, but DHT treatment seemed to little affect. Plasma aldosterone levels were also increased by ACTH injection, and there were no differences between cho- and DHT treated goats at 15 and 30 min after the ACTH injection. However, when goats were given the lower doses of ACTH (0.02 and 0.005 mg), plasma aldosterone levels were restored rapidly only in cho-treated goats, whereas those in DHT-treated goats were maintained throughout the 60 min experimental period. Consequently, plasma aldosterone levels in DHT-treated goats were higher than those in cho-treated goats at 45 and 60 min. One possible mechanism of the effect of DHT on the ACTH-induced increase in aldosterone synthesis may be the reduction of the activity of P450-17α, that is the enzyme to convert pregnenolone to 17α-OH-pregnenolone, and this mechanism may also be responsible to the suppressive effect of DHT on the ACTH-induced Cor synthesis.

KEY WORDS: ACTH, aldosterone, androgen, cortisol, goat.

J. Vet. Med. Sci. 71(3): 281–285, 2009

Our previous works reported that the increase in plasma cortisol (Cor) levels during road transportation, which can be a severe stress to domestic animals including goats [3, 12, 14], were significantly reduced by testosterone (T) or 5α-dihydrotestosterone (DHT) treatments in castrated male goats [1, 2]. We further demonstrated that androgen treatment reduced the transportation-induced increase in plasma Cor levels even when increase in plasma ACTH levels were not affected [1], and that androgen treatment reduced the increase in plasma Cor levels induced by adrenocorticotropic hormone (ACTH) administration in goats [13]. This report indicates that the suppression of transportation-induced increase in Cor secretion by androgen in goats is mainly a result of the suppression of the response of the adrenal cortex to ACTH, although androgen can affect Cor secretion by acting in the hypothalamus and/or the pituitary levels in some part [7].

The similar suppressions of the ACTH-induced secretion of glucocorticoid by androgen were also reported in experimental rodents [16], sheep [19] and cattle [4]. In rats and mice, the biological mechanisms of the effects of androgen on the response of adrenal cortex to ACTH have been investigated. The expression levels of adrenal ACTH receptor mRNA is decreased by T treatment in castrated rats [21]. While in mice, T decreased the immunoreactive protein, mRNA and activity of 3β-hydroxysteroid dehydrogenase-isomerase, that is one of the enzymes relates the production of adrenal steroid, in the adrenal gland [18]. These reports indicate that androgen may act on the various process of adrenal steroid production. It is need to examine the mechanisms of the suppressive effects of androgen on the caprine adrenal gland.

Three types of steroid hormones, those are glucocorticoids, adrenal androgen and mineralocorticoids, are secreted from the adrenal cortex. Similar to glucocorticoids, the secretion of adrenal androgen, such as dehydroepiandrosterone (DHEA) and androstenedione, are stimulated by ACTH [9]. Mineralocorticoids, such as aldosterone, play the significant roles in the regulation of water and sodium contents in the body [17]. The major stimulating hormone for aldosterone is angiotensin II, but ACTH also stimulates its secretion in some degree [5, 11, 15].

It is possible that androgen affect not only the ACTH-induced secretion of Cor but also adrenal androgen and/or aldosterone because all steroid hormones are synthesized from cholesterol through a certain biosynthetic pathway [6]. In rats, similar to corticosterone, ACTH-induced secretion of aldosterone is also reduced by androgen [8]. However, in ruminants, the effects of androgen on the secretion of adrenal androgen and/or mineralocorticoids are not known. The mechanisms of the suppressive effect of androgen on

* CORRESPONDENCE TO: AOYAMA, M., Laboratory of Function and Morphology, Department of Animal Science, Faculty of Agriculture, Utsunomiya University, 350 Minemachi, Utsunomiya-Shi, 321-8505, Japan.
e-mail: aoyamam@cc.utsunomiya-u.ac.jp

**PRESENT ADDRESS: MAEJIMA, Y., Department of Physiology, School of Medicine, Jichi Medical University, 3311–1 Yakushiji Shimotsuke-Shi, 329–0498, Japan.

ACTH-induced secretion of Cor in goats might be inferred by investigating the effects on other hormones from the adrenal cortex. In this study, we investigated the effects of DHT treatment on the ACTH-stimulated secretion of androstenedione and aldosterone, as well as Cor, in castrated male goats.

MATERIALS AND METHODS

Animals: Four castrated male Shiba goats (25–33 kg, 4–6 years old) were obtained from the experimental station of the University of Tokyo. They were castrated at least six months prior to the experiment. Usually, they were housed in the research farm of the Faculty of Agriculture, Utsunomiya University. At least seven days prior to the experiment, the animals were kept in the experimental room. Animals were loosely tied to individual stanchions and kept under a constant daylight cycle (light on 7:00–19:00 hr) and temperature (22–23°C). They were fed daily with *ad libtum* lucerne hay and 100 g of pelleted diet (ZC: Oriental Yeast Co., Ltd., Tokyo, Japan), and water was always available. The lucerne hay and water were changed to the new one, and the cage was cleaned every day at 13:00.

Androgen treatment: Administration of androgens was carried out as described by Aoyama *et al.* [1, 2]. Each goat received hormone treatment 9 to 14 days prior to the experiment. Three silicon capsules (made from silicon sheets 70 × 50 mm, 0.5 mm thickness: Tigers Polymer, Osaka, Japan), containing 0.8 g of 5α-dihydrotestosterone (DHT) (Wako Pure Chemical Industries, Osaka, Japan), were implanted in subcutaneous into each animal. Capsules containing cholesterol (cho) (Wako) were used as a control. One capsules containing cho were implanted into each animal as a same manner with DHT. At the end of a series of the ACTH administration that is described below, the implanted hormone was changed and the procedure was repeated. The order of the hormone treatments in two goats was cho-DHT but it was DHT-cho in other two. The interval between hormone treatments was three weeks.

ACTH administration: One or two days before the start of the experiment, a catheter was fitted to the jugular vein for blood sampling and intravenous injection of ACTH. On the day of the experiment, 800 μL of sterile saline containing 0.005, 0.02 or 0.1 mg of ACTH (1–24) (tetracosactide acetate) (Cortrosyn; Daiichi Pharmaceuticals, Tokyo, Japan) were injected into the jugular vein through the catheter at 16:00 hr. Three ACTH doses that were described above were challenged to each goat, and the interval among the injection of each dose was more than three days. The order of the injected dose was randomised.

Blood sampling: Five mL of blood samples were collected at 15:30, 16:00 (just before the ACTH injection), 16:15, 16:30, 16:45 and 17:00 hr. The plasma samples were separated by centrifugation (3000 rpm, 4°C, 10 min).

Assays: The concentrations of the adrenal hormones were measured by radioimmunoassay.

For assays for Cor and androstenedione, these hormones were extracted from the plasma with the following procedure. Two mL of diethyl ether was added to 500 μL of plasma, and mixed vigorously for 30 sec, and then the plasma layer was frozen at –80°C. The ether layer was moved to another tube by decantation and was evaporated with centrifuge (3,000 rpm) under the vacuum condition. This procedure was repeated twice. The extracted substances were reconstituted with 500 μL of 0.01 M phosphate buffer (pH 7.5) containing 0.14 M NaCl, 0.1% gelatin and 0.1% sodium aside (Gel-PBS). These extracted samples were stored at –30°C.

For Cor assay, 10 μL of each extracted sample was adjusted to a total volume of 300 μL by Gel-PBS. Then 100 μL of antibody against cortisol (FKA-404; Cosmo Bio Co., Ltd., Tokyo, Japan) that was diluted (1:5,000) with 0.01 M phosphate buffer containing 0.14 M NaCl, 0.05 M EDTA and 0.1% sodium aside (EDTA-PBS), and 100 μL of [3H]-labeled hydrocortisone (NET-396; Perkin Elmer Inc, Waltham, MA) that was adjusted to 20,000 dpm per tube with Gel-PBS, were added to each sample and incubated for 36–48 hr at 4°C. After the incubation, 250 μL of dextran-coated charcoal solution (DCC), that was the 0.01 M phosphate buffer containing 0.14 M NaCl, 0.05% dextran (Dextran T-70; Pharmacia Corporation, Peapack, NJ) and 0.5 % charcoal (Norit sx-3; Wako), was added to per tube and further incubated for 20 min at 4°C. Then DCC was separated by centrifuge (3,000 rpm, 4°C, 15 min), and supernatant was moved to assay tube and mixed with 2 mL of scintillation fluid (Clearsol I; Nacalai Tesque, Kyoto, Japan), and then the radioactivity was measured with a scintillation counter (LSC-6100; Aloka Co., Ltd., Tokyo, Japan).

For androstenedione assay, 200 μL of each extracted-sample was adjusted to a total volume of 300 μL by Gel-PBS. Then each sample was incubated with 100 μL of antibody against androstenedione (FKA-138; Cosmo Bio) (dilution 1:10,000) and 100 μL of [3H]-labeled androstenedione (NET-469; Perkin Elmer) (10,000 dpm per tube) for 24 hr at 4°C. After the incubation, the plasma androstenedione level was measured with the same manner as Cor assay.

Plasma aldosterone levels were measured using a commercially available radioimmunoassay kit (DPC aldosterone kit; Diagnostic Product Co., Los Angeles, CA). Normal plasma was used for the aldosterone assay.

Data analysis: In order to examine the effects of ACTH injection on the plasma levels of each adrenal hormones, the difference among the sampling points within the same ACTH dose and the same hormone treatment were compared using repeated measures analysis of variance (ANOVA) (animals × sampling point) and Tukey's test.

In order to examine the effects of DHT treatment, the differences between cho and DHT treatment within the same sampling point and the same ACTH dose were compared with repeated measures ANOVA (animals × hormone treatment).

P values less than 0.05 were considered as significant.

RESULTS

Cortisol: Regardless of the presence or absence of DHT treatment, plasma Cor levels were increased by all doses ACTH injection, and the high levels of plasma Cor were maintained for 60 min (Fig. 1). Plasma Cor levels between 15 and 60 min point (after ACTH injection) were significantly higher than the data at 0 min (just before the ACTH injection) in all ACTH doses in both treatments. There were no differences in the basal levels of plasma Cor (at –30 and 0 min point) between cho- and DHT-treated goats, but after the ACTH injection, those in DHT-treated goats were significantly lower than those in cho-treated goats throughout the 60 min experiment when goats were given 0.1 and 0.02 mg of ACTH (Fig. 1B, C). When goats were given 0.005 mg of ACTH, plasma Cor levels in DHT-treated goats tended to be lower than those in cho-treated goats although it was not statistically significant (Fig. 1A).

Androstenedione: Plasma levels of androstenedione in DHT-treated goats were higher than those in cho-treated goats at –30 and 0 min, before the ACTH injection (Fig.2 A, B, C). The anti-androstenedione antibody used in this study cross-react with 1.23% of DHT, thus the plasma androstenedione level might be overestimated in DHT-treated goats. Therefore, the averaged value at –30 and 0 min was regarded as the basal level, and the difference from the basal level within each test was regarded as the effect of ACTH (Fig.2 D, E, F). Plasma androstenedione levels between 15 and 60 min point were significantly higher than the data at 0 min excepting in DHT-treated goats given 0.005 mg ACTH, in which plasma androstenedione levels tended to be increased by ACTH but it didn't reach to the statistical sig-

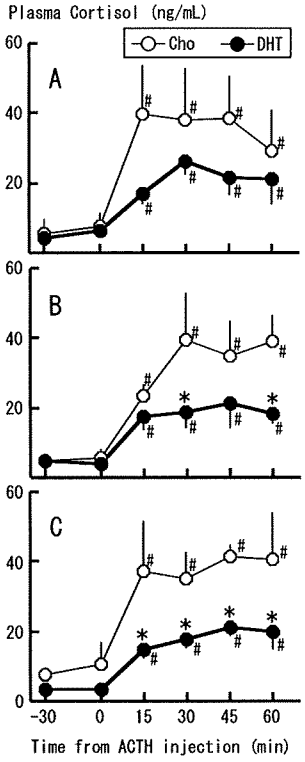

Fig. 1. Effects of androgen on the increases in plasma levels of cortisol induced by different doses (A: 0.005 mg, B: 0.02 mg, C: 0.1 mg per animal) of adrenocorticotropic hormone (1–24) administration in castrated male goats. Data were represented as the mean ± SE of four goats. Cho: cholesterol, DHT: 5α-dihydrotestosterone. #: Significantly different from the data at 0 min within the same hormone treatment ($P<0.05$; repeated measures analysis of variance and Tukey's test), *: significantly different from cho-treated goats at the same time point ($P<0.05$; repeated measures analysis of variance).

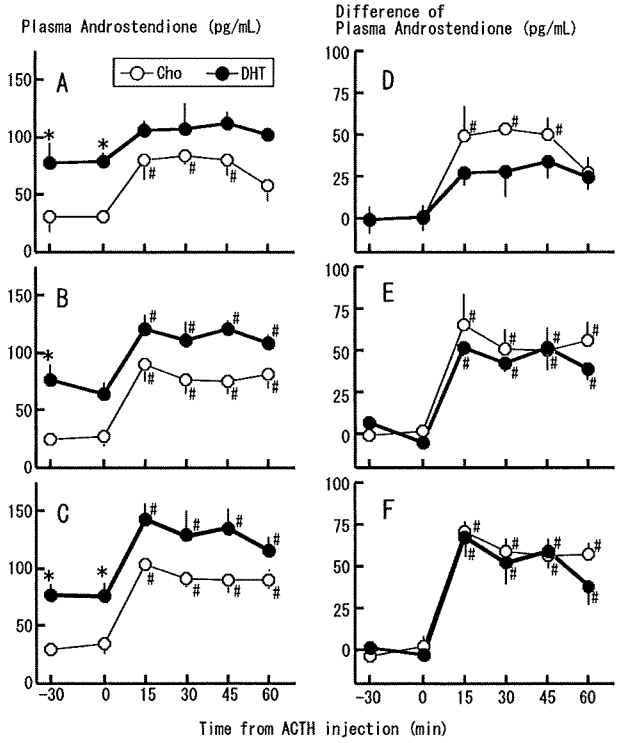

Fig. 2. Effects of androgen on the increases in plasma levels of androstenedione induced by different doses (A and D: 0.005 mg, B and E: 0.02 mg, C and F: 0.1 mg per animal) of adrenocorticotropic hormone (1–24) administration in castrated male goats. Data were represented as the mean ± SE of four goats. Panel A, B and C represent the original data, and panel D, E and F are represented as the difference from the basal level (defined as the averaged value of –30 and 0 min point) in each treatment. Cho: cholesterol, DHT: 5α-dihydrotestosterone. #: Significantly different from the data at 0 min within the same hormone treatment ($P<0.05$; repeated measures analysis of variance and Tukey's test), *: significantly different from cho-treated goats at the same time point ($P<0.05$; repeated measures analysis of variance).

nificance (Fig. 2D, E, F). Although the plasma androstenedione levels in DHT-treated goats given 0.005 mg of ACTH tended to be lower than those in cho-treated goats, there was no difference in plasma androstenedione levels between cho- and DHT-treated goats.

Aldosterone: Plasma aldosterone levels between 15 and 60 min point were significantly higher than the data at 0 min in all ACTH doses in both treatments (Fig. 3). However, in cho-treated goats given the lower ACTH doses (0.02 and 0.005 mg), plasma aldosterone levels began to decrease within 30 min (Fig. 3A, B), and especially in goats given 0.005 mg of ACTH, plasma aldosterone level at 60 min did not differ from that at 0 min anymore (Fig. 3A). These rapid restores of plasma aldosterone levels were not seen in DHT-treated goats. When goats were given 0.02 and 0.005 mg of ACTH, plasma aldosterone levels in DHT-treated goats were significantly higher than those in cho-treated goats at 45 and 60 min point (Fig. 3A, B). In 0.1 mg of ACTH injection, plasma aldosterone levels in cho- and DHT-treated goats did not differ throughout the 60 min experimental period (Fig. 3C).

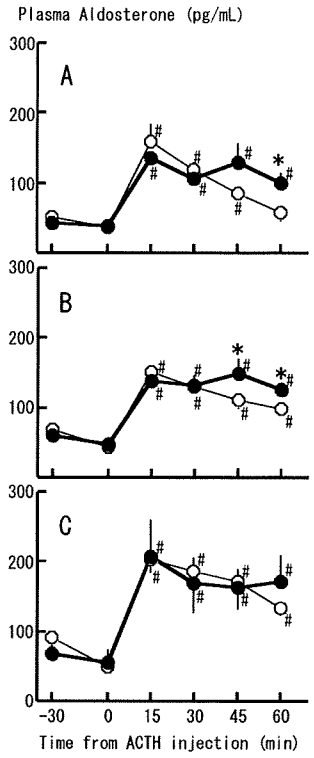

Fig. 3. Effects of androgen on the increases in plasma levels of aldosterone induced by different doses (A: 0.005 mg, B: 0.02 mg, C: 0.1 mg per animal) of adrenocorticotropic hormone (ACTH) (1–24) administration in castrated male goats. Data were represented as the mean ± SE of four goats. Cho: cholesterol, DHT: 5α–dihydrotestosterone. #: Significantly different from the data at 0 min within the same hormone treatment ($P<0.05$; repeated measures analysis of variance and Tukey's test), *: significantly different from cho-treated goats at the same time point ($P<0.05$; repeated measures analysis of variance).

DISCUSSION

In this study, DHT treatment reduced the levels of the ACTH-induced increase in plasma Cor in goats. This result agrees with our previous report [13]. In the lowest ACTH dose test (0.005 mg), one cho-treated goat had showed the smaller increase in plasma Cor level in the lowest ACTH dose, and this is why the difference between cho- and DHT-treated goats failed to be statistical significant. However, other three goats had showed the greater increase in plasma Cor level even when they were given the lowest ACTH dose during cho-treatment. It seems that DHT treatment suppress the increase in plasma Cor level induced by the lowest ACTH dose, as well as other two doses (0.02 and 0.1 mg), although it did not reach to statistical significance.

In this study, plasma Cor levels were increased within 15 min by ACTH injection, and these levels were maintained throughout the 60 min experimental period. DHT treatment decreased these maintained levels of plasma Cor. Since the maximum levels of plasma Cor were decreased by DHT treatment, androgen may reduce the rate of the limiting step for Cor synthesis. Androgen may decrease the reaction rate of a certain enzyme that relates to the step of the synthetic pathway of the steroid hormones; Stalvey reported that the activity of the 3β-hydroxysteroid dehydrogenase-isomerase, that is one of the enzymes related the production of adrenal steroid, was reduced by T in the mouse adrenal gland [18].

Plasma androstenedione levels were also increased by ACTH injection. Although the levels of androstenedione in DHT-treated goats tended to be lower than those of cho-treated goats when they were given 0.005 mg of ACTH, DHT treatment did not affect the ACTH-induced increase in plasma androstenedione levels. However, the effects of DHT on plasma androstenedione levels may not be regarded as the exact value. The antibody we used in this study cross-react with DHT 1.23%, thus the effect of DHT treatment on the androstenedione level might be masked by the higher level of plasma DHT in DHT-treated goats.

Similarly to other animals [5, 11, 15], ACTH increased also plasma aldosterone level in goats. Interestingly, unlike plasma Cor level, DHT treatment enhanced, rather than suppressed, the ACTH-induced increase in plasma aldosterone level. The aspects of the effects of ACTH injection on plasma aldosterone levels were different from those in Cor. The lower doses of ACTH injection (0.02 and 0.005 mg) increased plasma aldosterone levels within 15 min, but these levels began to decrease immediately only in cho-treated goats. While in DHT-treated goats, the increased levels of plasma aldosterone were maintained for 60 min. Consequently, plasma aldosterone levels did not differ between cho- and DHT-treated goats at 15 and 30 min point, but those in DHT-treated goats were higher than those in cho-treated goats at later half of the experiment. DHT treatment did not seem to affect the rate of the limiting step for aldos-

terone synthesis because the peak levels, which were seen at 15 min point, did not differ between cho- and DHT treated goats. One possible mechanism of the effect of DHT on the ACTH-induced increase in aldosterone synthesis is the reduction of the activity of P450-17α, that is the enzyme to convert pregnenolone to 17α-OH-pregnenolone (or progesterone to 17α-OH-progesterone). In cho-treated goats, pregnenolone and progesterone, which are the precursor of aldosterone, might be lost rapidly by the higher activation of P450-17α, and consequently, plasma aldosterone level might be decreased. DHT treatment might keep the high level of plasma aldosterone by reducing the activity of P450-17α.

If androgen decreases the activity of P450-17α, the suppressive effect of androgen on the ACTH-induced Cor synthesis might be a result of this effect at least partially. This hypothesis will be confirmed by examining the effect of androgen on the expression of P450-17α or their activity in the cultured adrenal cortical cells, like a previous work [6].

While, the effects of DHT on the ACTH-induced increase in plasma Cor and aldosterone levels may be the results of other biological mechanisms. For example, adrenal steroid hormone(s) can influence the secretion of other adrenal steroid hormones [20]. The enhancement of increase in plasma aldosterone level may be a result of the relatively lower level of plasma Cor instead of the directly effects of DHT. Otherwise, DHT might enhance the ACTH-induced increase in plasma aldosterone level by suppressing the metabolism of aldosterone. Latif *et al.* reported that the metabolism of aldosterone in the liver is influenced by other steroid hormones in rats [10]. The further researches are necessary to confirm the mechanisms of the effect of androgen on the steroid synthesis in the caprine adrenal glands.

In this study, we have found that androgen suppressed the ACTH-induced plasma Cor level but enhanced the ACTH-induced plasma aldosterone level in goats.

ACKNOWLEDGEMENT. We are grateful to Dr. Y. Nagao and the staff members of the research farm of the Utsunomiya University for their care of the animals.

REFERENCES

1. Aoyama, M., Maejima, Y., Keyaki, S., Muroi, M., Tohei, A. and Sugita, S. 2005. Effects of androgen on plasma levels of adrenocorticotropic hormone and cortisol during transportation in goats. *J. Vet. Med. Sci.* **67**: 1109–1114.
2. Aoyama, M., Negishi, A., Abe, A., Maejima, Y. and Sugita, S. 2003. Sex differences in stress response to transportation on goats: Effects of gonadal hormones. *Anim. Sci. J.* **74**: 511–519.
3. Aoyama, M., Negishi, A., Abe, A., Maejima, Y. and Sugita, S. 2008. Short-term transportation in a small vehicle affects the physiological state and subsequent water consumption in goats. *Anim. Sci. J.* **79**: 526–533.
4. Boissy, A. and Bouissou, F.M. 1994. Effects of androgen treatment on behavioral and physiological responses of heifers to fear-eliciting situations. *Horm. Behav.* **28**: 66–83.
5. Chavarri, M.R., Yamakita, N., Chiou, S. and Gomez-Sanchez, C.E. 1993. Calf adrenocortical fasciculata cells secrete aldosterone when placed in primary culture. *J. Steroid Biochem. Mol. Biol.* **45**: 493–500.
6. Engelbrecht, Y. and Swart, P. 2000. Adrenal function in angora goats: a comparative study of adrenal steroidogenesis in Angora goats, Boer goats, and Merino sheep. *J. Anim. Sci.* **78**: 1036–1046.
7. Handa, R.J., Nunley, K.M., Lorens, S.A., Louie, J.P., McGivern, R.F. and Bollnow, M.R. 1994. Androgen regulation of adrenocorticotropin and corticosterone secretion in the male rat following novelty and foot shock stressors. *Physiol. Behav.* **55**: 117–124.
8. Kau, M.M., Lo, M.J., Wang, S.W., Tsai, S.C., Chen, J.J., Chiao, Y.C., Yeh, J.Y., Lin, H., Shum, A.Y., Fang, V.S., Ho, L.T. and Wang, P.S. 1999. Inhibition of aldosterone production by testosterone in male rats. *Metabolism* **48**: 1108–1114.
9. Kramer, R.E., Buster, J.E. and Andersen, R.N. 1990. Differential modulation of ACTH-Stimulated cortisol and androstenedione secretion by insulin. *J. Steroid. Biochem.* **36**: 33–42.
10. Latif, S.A., McDermott, M.J. and Morris, D.J. 1983. The effects of adrenal and gonadal steroids and K^+-canrenoate on the metabolism of aldosterone by rat liver microsomes. *Steroids* **42**: 283–297.
11. Lehoux, J.G., Fleury, A. and Ducharme, L. 1998. The acute and chronic effects of adrenocorticotropin on the levels of messenger ribonucleic acid and protein of steroidogenic enzymes in rat adrenal *in Vivo*. *Endocrinology* **139**: 3913–3922.
12. Maejima, Y., Aoyama, A., Abe, A. and Sugita, S. 2005. Induced expression of c-fos in the diencephalon and pituitary gland of goats following transportation. *J. Anim. Sci.* **83**: 1845–1853.
13. Maejima, Y., Aoyama, M., Kobayashi, N. and Sugita, S. 2006a. Adrenocorticotropic hormone-induced secretion of cortisol in goats is inhibited by androgen. *Anim. Sci. J.* **77**: 87–94.
14. Maejima, Y., Aoyama, M. and Sugita, S. 2006b. Expression of c-fos-like immunoreactive cells in the adrenal gland following transportation stress in goats. *Small Rum. Res.* **63**: 162–169.
15. Müller, J.1998. Regulation of aldosterone biosynthesis: the end of the road? *Clin. Exp. Pharmacol. Physiol. (Suppl.)* **25**: S79–S85.
16. Nowak, W.K., Neri, G., Nussdorfer, G.G. and Malendowicz, K.L. 1995. Effect of sex hormones on the steroidogenic activity of dispersed adrenocortical cells of the rat adrenal cortex. *Life Sci.* **57**: 833–837.
17. Pocock, G. and Richards, C.D. 2004. The regulation of body fluid volume. pp. 611–627. *In*: Human Physiology: The Basis of Medicine Second Edition. Oxford University Press, Oxford.
18. Stalvey, D.R.J. 2002. Inhibition of 3β-hydroxysteroid dehydrogenase-isomerase in mouse adrenal cells: a direct effect of testosterone. *Steroids* **67**: 721–731.
19. Turner, A.L., Canny, B.J., Hobbs, R.J., Bond, J.D., Clarke, I.J. and Tilbrook, A.J. 2002. Influence of sex and gonadal status of sheep on cortisol secretion in response to ACTH and on cortisol and LH secretion in response to stress: importance of different stressors. *J. Endocrinol.* **173**: 113–122.
20. Vecseiweisz, P., Farkas, K., Kemeny, V. and Harangozo, M. 1965. Investigations on the mechanisms of reduced aldosterone production caused by the administration of hydrocortisone. *Steroids* **5**: 415–421.
21. Yoshimura, S., Sakamoto, S., Kudo, H., Sassa, S., Kumai, A. and Okamoto, R. 2003. Sex differences in adrenocortical responsiveness during development in rats. *Steroids* **68**: 439–445.

Effects of Medial Hypothalamic Lesions on Feeding-Induced Entrainment of Locomotor Activity and Liver *Per2* Expression in *Per2*::luc Mice

Yu Tahara,[*] Akiko Hirao,[*] Takahiro Moriya,[†] Takashi Kudo,[‡] and Shigenobu Shibata[*,1]

[*]*Department of Physiology and Pharmacology, School of Advanced Science and Engineering, Waseda University, Tokyo, Japan,* [†]*Department of Cellular Signaling, Graduate School of Pharmaceutical Sciences, Tohoku University, Sendai, Japan, and* [‡]*Department of Psychiatry, University of California–Los Angeles, Los Angeles, CA*

Abstract Restricted feeding induces anticipatory activity rhythm and also entrains the peripheral circadian clocks, although the underlying brain mechanisms have not been fully elucidated. The dorsomedial hypothalamus (DMH) has been implicated in the regulation of restricted feeding–induced anticipatory activity rhythms (FAA), but the role of the DMH in restricted feeding–induced entrainment of peripheral circadian clocks is still unknown. In the present study, the role of the DMH in entrainment of the peripheral circadian clock was examined using *Per2*::luciferase knock-in mice. The results indicate that lesions that destroy the large mediobasal hypothalamic (MBH) lesions destroying the DMH, ventrolateral hypothalamus (VMH), and arcuate nucleus (ARC) significantly reduce daily locomotor activity rhythms and FAA formation. In addition, these lesions phase advanced the peak of liver *Per2* expression by 2 h when compared to sham-operated mice. Following the administration of MBH lesions, the animals run less and start later in the restricted feeding–induced FAA rhythm but do not have any alterations in the restricted feeding–induced phase shift of the liver *Per2* rhythm. These results demonstrate that the hypothalamus, including the MBH, is an important brain area for maintaining the locomotor rhythm and FAA formation. However, it is not necessary for restricted feeding–induced entrainment of the liver clock.

Key words food anticipatory activity, clock gene, feeding rhythm, liver, dorsomedial hypothalamus, suprachiasmatic nucleus

Food anticipatory activity (FAA) is characterized by locomotor activity that increases 2 to 3 h before restricted feeding time. Putative brain areas that regulate this behavior are hypothalamic regions that are central to the regulation of energy homeostasis and arousal, including the arcuate nucleus (ARC), paraventricular nucleus (PVN), dorsomedial hypothalamus (DMH), and ventromedial hypothalamus (VMH) (Cone et al., 2001; Rodgers et al., 2002; Saper et al., 2005a, b; Ribeiro et al., 2007; Poulin and Timofeeva, 2008).

1. To whom all correspondence should be addressed: Shigenobu Shibata, Department of Physiology and Pharmacology, School of Advanced Science and Engineering, Waseda University, Wakamatsu-cho 2-2, Shinjuku-ku, Tokyo 162-8480, Japan; e-mail: shibatas@waseda.jp.

JOURNAL OF BIOLOGICAL RHYTHMS, Vol. 25 No. 1, February 2010 9-18
DOI: 10.1177/0748730409352782

The persistence of a behavioral FAA rhythm following electrolytic or thermal lesions of the DMH has been reported in rats (Landry et al., 2006, 2007) and mice (Moriya et al., 2009). Conversely, Gooley et al. (2006) reported that cell-specific lesions of the DMH attenuated restricted feeding–induced FAA and body temperature rhythms in rats. The authors reported a correlation between the number of remaining cells and the magnitude of FAA and inferred that FAA would be absent if all of the cells of the DMH were destroyed. Thus, the role of the DMH on FAA maintenance remains unclear.

Daily restricted feeding can also entrain peripheral circadian clocks. Clock gene rhythms in the liver and cerebral cortex can be entrained by restricted feeding stimuli, even when suprachiasmatic nucleus (SCN) activity remains locked to the light-dark (LD) cues or when the SCN is ablated (Damiola et al., 2000; Stokkan et al., 2001; Hara et al., 2001; Wakamatsu et al., 2001, Moriya et al., 2009). Dissociations between behavioral FAA rhythms and those of peripheral clock gene expression have previously been reported. Feillet et al. (2006) demonstrated that *Per2* mutant mice exhibit weak FAA rhythms but exhibit a strong phase shift of peripheral clock gene expression. Davidson et al. (2003) also reported that fasting re-established FAA in mice that are offered *ad libitum* feeding for 1 week after establishment of an FAA rhythm. However, these mice did not show a phase change of peripheral clock gene expression rhythm under a re-established FAA. The role of the DMH in restricted feeding–induced entrainment of peripheral circadian clocks, however, has not been explored.

To address this question, we examined whether clock gene rhythm in the liver of mice with MBH lesions can be entrained by restricted feeding stimuli. To do this, we used *Per2*::luc knock-in mice to monitor *Per2* gene expression in the liver.

MATERIALS AND METHODS

General Conditions of Animals and Housing

Per2::luc knock-in mice (founders courtesy of Dr. Joseph Takahashi, Northwestern University) (Yoo et al., 2004) were bred in house. For the mouse experiments, we used *Per2*::luc homozygous and heterozygous male mice weighing 25 to 35 g each. We saw no differences in peak time of bioluminescence between homozygous and heterozygous mouse livers (17.9 ± 0.32 o'clock for homozygous, $N = 7$; 18.1 ± 0.26 o'clock for heterozygous, $N = 8$). The animal room had a controlled temperature of 22 ± 2 °C, humidity of 60% ± 5%, and a 12-h light/12-h dark cycle (i.e., lights-on from 0800 to 2000 h). Zeitgeber time ZT0 and ZT12 were the lights-on and lights-off times, respectively. The light intensity at the surface of the cages was approximately 100 lux. Prior to the restricted feeding experiment, mice were fed commercial normal rodent chow (Catalog #MF, Oriental Yeast Co. Ltd., Tokyo, Japan), and water was available *ad libitum*. Experimental animal care was conducted under the permission of the Animal Welfare Committee of Waseda University (Permission #09A11).

Locomotor Activity Analysis and Index of Anticipatory Activity

Mice were housed individually during restricted feeding. General locomotor activity was recorded with an infrared radiation sensor (F5B, Omron, Tokyo, Japan) and analyzed with CLOCKLAB software (Actimetrics, Wilmette, IL). Analysis of activity was measured as the number of the sensor counts per 6 min. Percentage change in activity before and after restricted feeding was calculated by the following formula: 100 × (1-h bin activity / daily total 24-h activity). The strength of anticipatory activity was evaluated by comparison of mean percentage activity (ZT3-ZT6) or (ZT21-ZT0) during the last 3 days after a restricted feeding schedule and ZT3-ZT6 or ZT21-ZT0 during the 3 to 5 days before the restricted feeding schedule, respectively. We analyzed data segments of locomotor activity from day 5 to day 10 after administration of the MBH lesions by χ^2 periodograms. A range of 18 to 30 h was used to assess the period of rhythm and its robustness.

Surgery

Mice were anesthetized with ketamine (50 mg/kg administered i.p.) and positioned in a stereotaxic frame (Narishige Co., Tokyo, Japan) for the placement of stainless steel electrodes (0.35 mm in diameter) into the DMH. The stereotaxic coordinates were 0.8 mm posterior, ±0.3 mm lateral to the bregma, and 6.5 mm under the skull surface. Bilateral lesions were made with a thermal lesion device (RFG-4A, Muromachi, Tokyo, Japan) that heated the electrode tip to 55 °C for 4 sec via a current path. To avoid an incomplete lesion in the DMH area, we created a relatively large lesion area in the ventral and dorsal portions of the medial hypothalamus in comparison with our previous paper (Moriya et al., 2009). Thus,

we created lesions within the medial parts of the hypothalamus including the DMH. Sham-operated mice were treated in the same manner but without the current path. All mice were given 10 days to recover from surgery in LD with *ad libitum* food access.

Brain Staining and Verification of Lesion Site

The brains of all animals with lesions were collected after the mice were sacrificed for bioluminescence experiments under ether anesthesia. The brains were stored in 4% paraformaldehyde for 3 to 4 days; 60-μm serial coronal sections from sham and MBH-lesioned mice were then stained with cresyl violet and photographed through the SCN and DMH area using a digital camera attached to a light microscope (BX51, Olympus, Tokyo, Japan). The borders of the DMH, VMH, and ARC were drawn on the digital images by referencing a mouse brain atlas (*The Mouse Brain in Stereotaxic Coordinates, 2nd ed.*; G Paxinos and KBJ Franklin, Academic Press, San Diego, CA). Mice with an incomplete lesion in the DMH area were excluded from the data (9/31 mice).

Restricted Feeding Shift Schedule

After 10 days of recovery from the surgery, mice were exposed to food deprivation for one night (starting at ZT10). After fasting, mice from the RF group were allowed access to food for 4 h, from ZT6 to ZT10 or from ZT0 to ZT4, for 7 consecutive days. On the eighth day, the mice were sacrificed at ZT3.

Preparation and Measurement of Bioluminescence from *Per2*::luc Mice

Following the feeding experiment, *Per2*::luc knock-in mice were sacrificed at ZT3 for recordings of bioluminescence rhythm in the liver. The liver was rapidly removed from the mouse and placed in ice-cold Hanks' balanced salt solution (pH 7.2; Sigma-Aldrich, St. Louis, MO). Liver tissues were cut into pieces, explanted into a 35-mm Petri dish (Iwaki & Co., Ltd., Chiba, Japan), sealed with parafilm (Sigma-Aldrich), and cultured with 1.3 mL of Dulbecco's Modified Eagle Medium (DMEM) (Invitrogen, Carlsbad, CA) supplemented with $NaHCO_3$ (2.7 mM), HEPES (10 mM), kanamycin (20 mg/L; Sigma-Aldrich), insulin (5 μg/mL; Sigma-Aldrich), putrescine (100 μM; Sigma-Aldrich), human transferrin (100 μg/mL; Sigma-Aldrich), progesterone (20 nM; Sigma-Aldrich), sodium selenite (30 nM; Sigma-Aldrich), and 0.1 mM D-luciferin sodium salt (Invitrogen, Carlsbad, CA). The cultures were incubated at 37 °C, and bioluminescence was monitored for a duration of 1 min at 10-min intervals with a dish-type luminometer (LumiCycle, Actimetrics).

Assessment of Circadian Periods and Liver Clock Phases

Raw data (1-min bins) were smoothed by an adjusting-averaging method with 2-h running means as previously described (Hayasaka et al., 2007; Ohta et al., 2008). The data were then detrended by subtracting the 24-h running average from the raw data using R software (R Development Core Team, http://www.r-project.org/), created by Mr. Tuyoshi Yaita and Dr. Shigenobu Shibata (Waseda University, Tokyo, Japan). Peaks were defined as a point at which bioluminescence was higher compared to adjacent points and confirmed by wave form. The peak phase time was evaluated by the second peak. The period of *Per2*::luc activity (recorded from 24 to 72 h in vitro) was assessed for each liver culture and calculated by averaging the period between the second and third peaks and the third and fourth peaks, respectively.

Statistical Analysis

The values are expressed as means ± standard errors of the mean. For statistical analysis, a 1-way or 2-way analysis of variance (ANOVA) using StatView software (SAS Institute, Cary, NC) was applied, and a post hoc analysis was conducted with a Student *t*-test or a Fisher protected least significant difference (PLSD) test.

RESULTS

Effect of MBH Lesions on Activity and Liver Bioluminescence Rhythms

MBH lesions attenuated the daily rhythm of locomotor activity (Figures 1A, 2A, and 3A) under an LD cycle. Although sham-operated mice showed a significant day/night difference of locomotor activity (Student *t*-test; $p < 0.01$), mice with MBH lesions did not show a significant difference (Figure 1B). MBH lesions did not affect the volume of daily food intake (1.4 ± 0.09 g/10 g B.W. for sham-operated mice, 1.31 ± 0.05 g/10 g B.W. for MBH-lesioned mice) but caused a slight increase in body weight (98.7% ± 0.2% change in sham-operated mice before the operation,

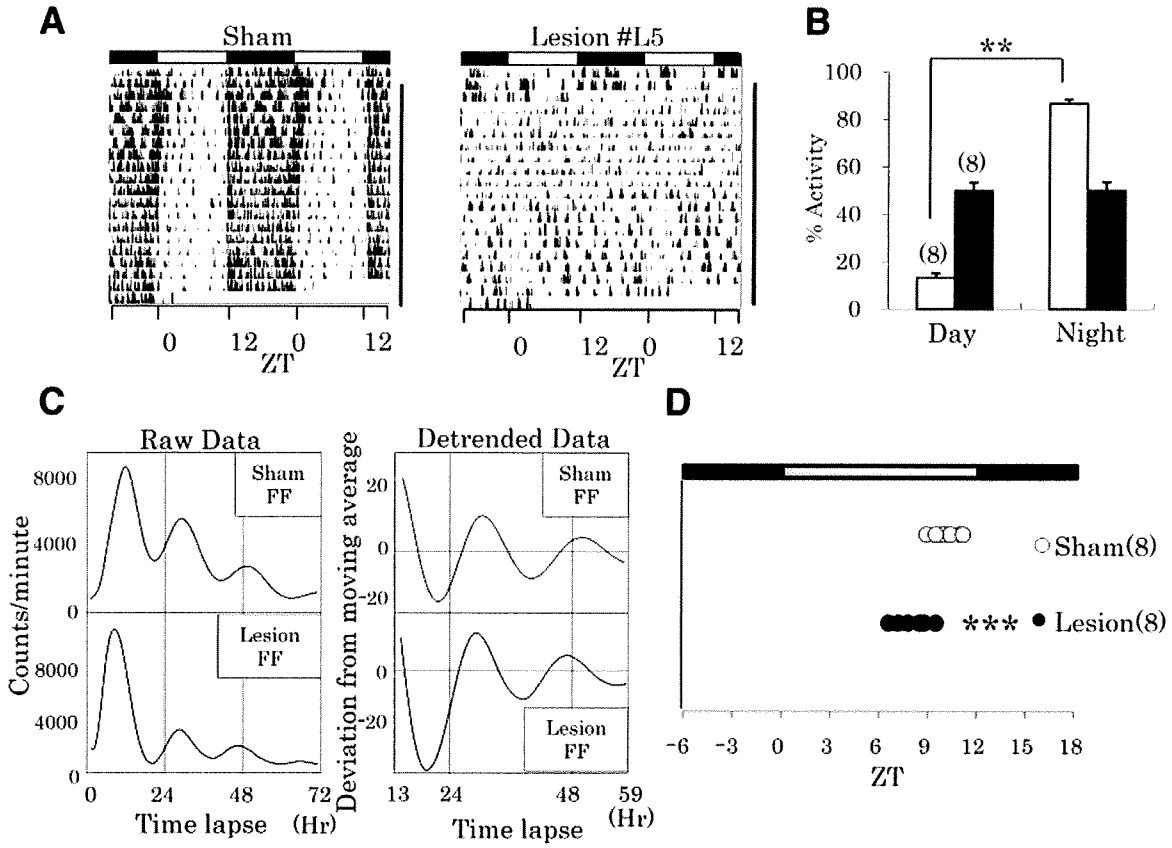

Figure 1. Effect of MBH lesions on locomotor activity and liver *Per2* rhythms. (A) Examples of double-plotted actograms of sham-operated or MBH-lesioned mice. The axis bar in each graph indicates the day path after surgery. Horizontal open and closed bars indicate the light and dark periods, respectively. Zeitgeber time (ZT) 0 indicates lights-on, and ZT12 indicates lights-off. (B) Day-night ratio (100%) of daily activity. After the 10-day recovery period passed, locomotor activity counts during the next 6 days were calculated. White bar, sham-operated group; black bar, lesioned group. Numbers in parentheses refer to the number of mice. **$p < 0.01$ between day and night; Student *t*-test. (C) Experimental raw or detrended data of liver bioluminescence rhythm in sham-operated or MBH-lesioned mice under free-feeding (FF) conditions. Bioluminescence rhythm was obtained from *Per2*::luciferase knock-in mouse. (D) Bioluminescence rhythm phase of *Per2*::luciferase mouse livers. Mice were sacrificed 17 days after surgery. Horizontal numbers indicate the ZT. ***$p < 0.001$ from sham-operated mice; Student *t*-test.

116.3% ± 6.9% change in MBH-lesioned mice before the operation, Student *t*-test; $p < 0.05$). The χ^2 periodogram analysis revealed that only 3 of 22 MBH-lesioned mice sustained a significant 24-h rhythmicity of the locomotor activity, whereas all of the sham-operated mice ($N = 20$) maintained 24-h rhythmicity.

A representative of raw and detrended data of liver *Per2*::luciferase bioluminescence rhythm in sham-operated or MBH-lesioned mice is shown in Figure 1C. MBH lesions did not affect the amplitude or period of the bioluminescence rhythm in the liver. However, the phase was advanced by 1.9 h when compared to the sham-operated mice (Student *t*-test; $p < 0.001$) (Figure 1C and 1D). The free-running period of the liver clock was 18.1 ± 0.3 ($N = 8$) for sham-operated mice and 18.2 ± 0.3 ($N = 8$) for MBH-lesioned mice with no significant differences between the 2 groups.

In many cases, lesion sites were included in the part of VMH and ARC. Figure 4A shows a lesion area of #L5, in which representative locomotor activity rhythm was already shown (Figure 1A). As described in Figure 4A, the current surgical procedure never caused damage to the SCN or PVN. Thus, all of the SCN was intact even if the lesion site in the MBH area was large. Eight circle lines at each level of the DMH in the lower panel of Figure 4A show the border of the lesion area for all lesioned mice ($N = 8$). The DMH was almost completely destroyed in all of the mice.

Effect of MBH Lesions on Anticipatory Activity Rhythm and Liver Rhythm Induced by RF of ZT6-ZT10

Locomotor activity increased 2 to 3 h before the restricted feeding time in sham-operated mice (Figure 2A, #S9). In some MBH-lesioned mice, there was a small increase in daytime activity in the 3-h prefeeding interval, suggesting FAA (Figure 2A, #L14; change from 10.7% to 25.9%), while in other animals, there was no change in daytime activity in the prefeeding

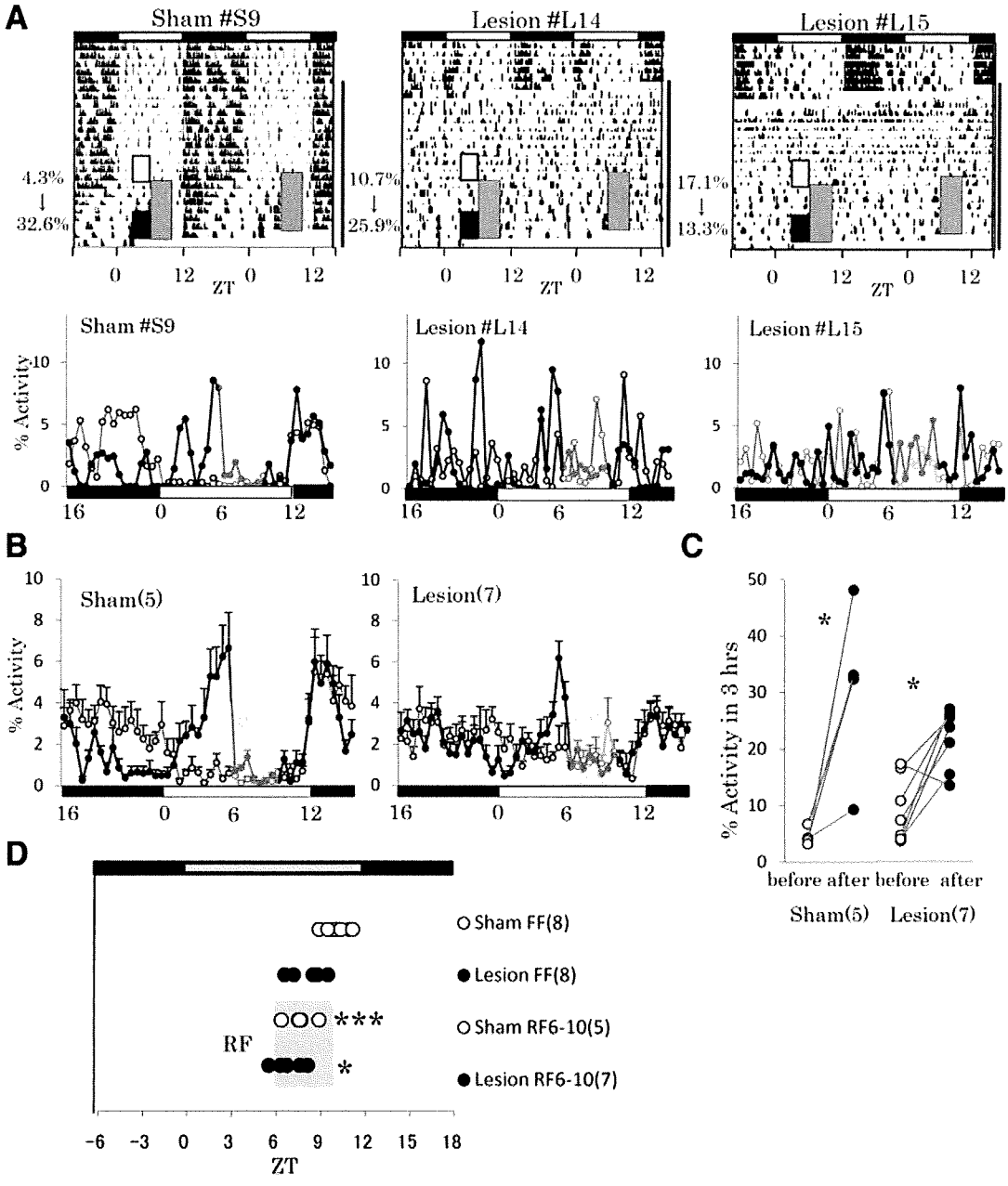

Figure 2. Effect of MBH lesions on restricted feeding (ZT6-ZT10)–induced food anticipatory activity rhythm and liver bioluminescence rhythms. (A) Examples of double-plotted actograms of sham-operated (#S9) or MBH-lesioned mice (#L14 and #L15) under a restricted feeding schedule. The axis bar in each graph indicates the day path after surgery. Horizontal open and closed bars indicate the light and dark periods, respectively. The restricted feeding time (gray rectangle box) was set at ZT6-ZT10 for 7 days after a 10-day surgery recovery period. Sham-operated mice (#S9) showed strong anticipation (change of percentage activity from 4.3% before [white rectangle box] to 32.6% after [black rectangle box]). Two representative examples of lesion mice are shown. Lesion #L15 shows almost no anticipation (change of percentage activity from 17.1% before [white rectangle box] to 13.3% after [black rectangle box]), but lesion #L14 shows moderate anticipation (change of percentage activity from 10.7% before [white rectangle box] to 25.9% after [black rectangle box]). In the lower panel of each sample, the mean daily percentage activity before (open circle) and after (closed circle) restricted feeding (gray rectangle box) is shown. (B) Percentage change of locomotor activity. Mean daily percentage activity of all mice before (open circle) and after (closed circle) restricted feeding (gray rectangle box) is shown. (C) Percentage activity was calculated by the following formula: 100 × (activity counts [ZT3-ZT6, hatched rectangle box in Figure 2A] / daily 24-h activity counts) during the last 3 days before (open circle) or after (closed circle) the restricted feeding schedule. Each circle in the figure indicates each specific sample. *$p < 0.05$ from before values (open circle); paired Student *t*-test. (D) Bioluminescence rhythm phase of *Per2*::luciferase mouse livers. Mice were sacrificed 8 days after a 7-day restricted feeding period (ZT6-ZT10). Data of sham-operated FF mice and MBH-lesioned FF mice were the same as in Figure 1D.

interval, and FAA was not detected (Figure 2A, #L15; change from 17.1% to 13.3 %). We showed the mean daily rhythm of percentage activity before and after restricted feeding in mouse example #S9, #L14, and #L15 (Figure 2A, lower panel) and in group data (Figure 2B). The start and run of FAA in MBH-lesioned mice were relatively lower and delayed in comparison with sham-operated mice (Figure 2B). We evaluated

the anticipatory activity increase by comparing the percentage change of activity counts during ZT3-ZT6 before and after restricted feeding (Figure 2C). The percentage change increased from 4.4% ± 0.6% to 31.1% ± 6.2% (paired Student *t*-test; $p < 0.05$) in the sham-operated mice and from 9.1% ± 2.2% to 21.6% ± 2.0% in the MBH-lesioned mice (paired Student *t*-test; $p < 0.05$) from restricted feeding, respectively. Consequently, the increase in activity during the period of FAA was 607% in sham-operated animals and 137% in the lesioned animals, resulting in a reduction of 77% in the activity increase of the animals. Restricted feeding of sham-operated mice during ZT6-ZT10 significantly advanced the liver *Per2* rhythm phase (1-way ANOVA; $F_{1,11} = 29.5$, $p < 0.001$) (Figure 3D). The same treatment to MBH-lesioned mice during ZT6-ZT10 also significantly advanced the liver *Per2* rhythm phase (1-way ANOVA; $F_{1,13} = 6.4$, $p < 0.05$). All animals showed a similar phase advance of the *Per2* liver rhythm irrespective of the lesion area (Figure 4B) and amount of FAA shown (Figure 2C). In Figure 4B, lesion areas of #L14 and #L15 are shown (upper panel). Seven circle lines at each level of the DMH in the lower panel of Figure 4B show the border of the lesion area for all lesioned mice ($N = 7$). DMH was almost completely destroyed in all mice.

Effect of MBH Lesions on Anticipatory Activity Rhythm and Liver Rhythm Induced by RF of ZT0-ZT4

Our data show that restricted feeding of MBH-lesioned mice during ZT6-ZT10 caused a small phase advance of liver *Per2* rhythm because the MBH lesion itself caused a phase advance of the liver rhythm. Thus, it is difficult to conclude that the MBH lesion had no effect on restricted feeding–induced phase advance of the liver clock. Therefore, in the next set of experiments, restricted feeding time was changed from ZT6-ZT10 to ZT0-ZT4. We showed the mean daily rhythm of percentage activity before and after restricted feeding in mouse sample #S18, #L20, and #L21 (Figure 3A, lower panel) and in group data (Figure 3B). Start time and size of FAA in MBH-lesioned mice were comparable with sham-operated mice (Figure 3B). We evaluated the anticipatory activity increase by comparing the percentage change of activity counts during ZT21-ZT0 before and after restricted feeding (Figure 3C). In sham-operated mice, percentage locomotor activity during ZT21-ZT0 was high before restricted feeding as well as after restricted feeding (Figure 3A and 3B). Thus, there were no significant differences of percentage activity between the before and after restricted feeding groups in the sham-operated mice (Figure 3C). As the percentage activity during ZT21-ZT0 in MBH-lesioned mice was relatively low, a significant increase of activity during ZT21-ZT0 was observed after restricted feeding treatment (paired Student *t*-test, $p < 0.01$) (Figure 3C). Restricted feeding for ZT0-ZT4 strongly and significantly advanced the phase of liver *Per2* rhythm in both sham-operated and MBH-lesioned mice (Figure 3D). There are no significant differences of phase shift between sham and ablation groups. MBH ablation #L20 showed increased anticipatory activity, but #L21 did not (Figure 3A). However, both samples exhibited a similar phase advance of *Per2* rhythm and had similar lesion areas (Figure 4C). The lesion areas of #L20 and #L21 are shown in Figure 4C. Seven circle lines at each level of the DMH in the lower panel of Figure 4C show the border of the lesion area for all lesioned mice ($N = 8$). The DMH was almost completely destroyed in all of the mice.

DISCUSSION

The first important finding of this study is that the widespread destruction of medial hypothalamic nuclei, including the DMH, and some parts of the VMH and ARC, does not affect the restricted feeding–induced phase advance of clock gene rhythm in the liver. In the SCN-lesioned mice, restricted feeding induced a phase advance of the liver clock in a similar manner as the intact mouse (Hara et al., 2001). Both SCN-lesioned (Hara et al., 2001) and MBH-lesioned mice (present result) showed the attenuation of locomotor activity rhythm. Taken together with the present results, it appears that the SCN-DMH pathway may not be involved in restricted feeding–induced phase shift of the liver clock, although this pathway may be critical for circadian rhythms of locomotor activity and feeding (Chou et al., 2003; Gooley et al., 2006).

Because there are conflicting reports about the role of the DMH in the establishment of FAA rhythm (Gooley et al., 2006; Landry et al., 2006, 2007; Moriya et al., 2009), we made large lesions in the MBH areas. This approach represents a strength of the study because it increases confidence of complete DMH ablation. In addition, it allows for the conclusion that the MBH circuits that regulate metabolism and ingestive behavior are not required for entraining circadian clocks in the liver to scheduled daytime meals.

In the present study, we employed 2 restricted feeding schedules: during ZT6-ZT10 and during ZT0-ZT4.

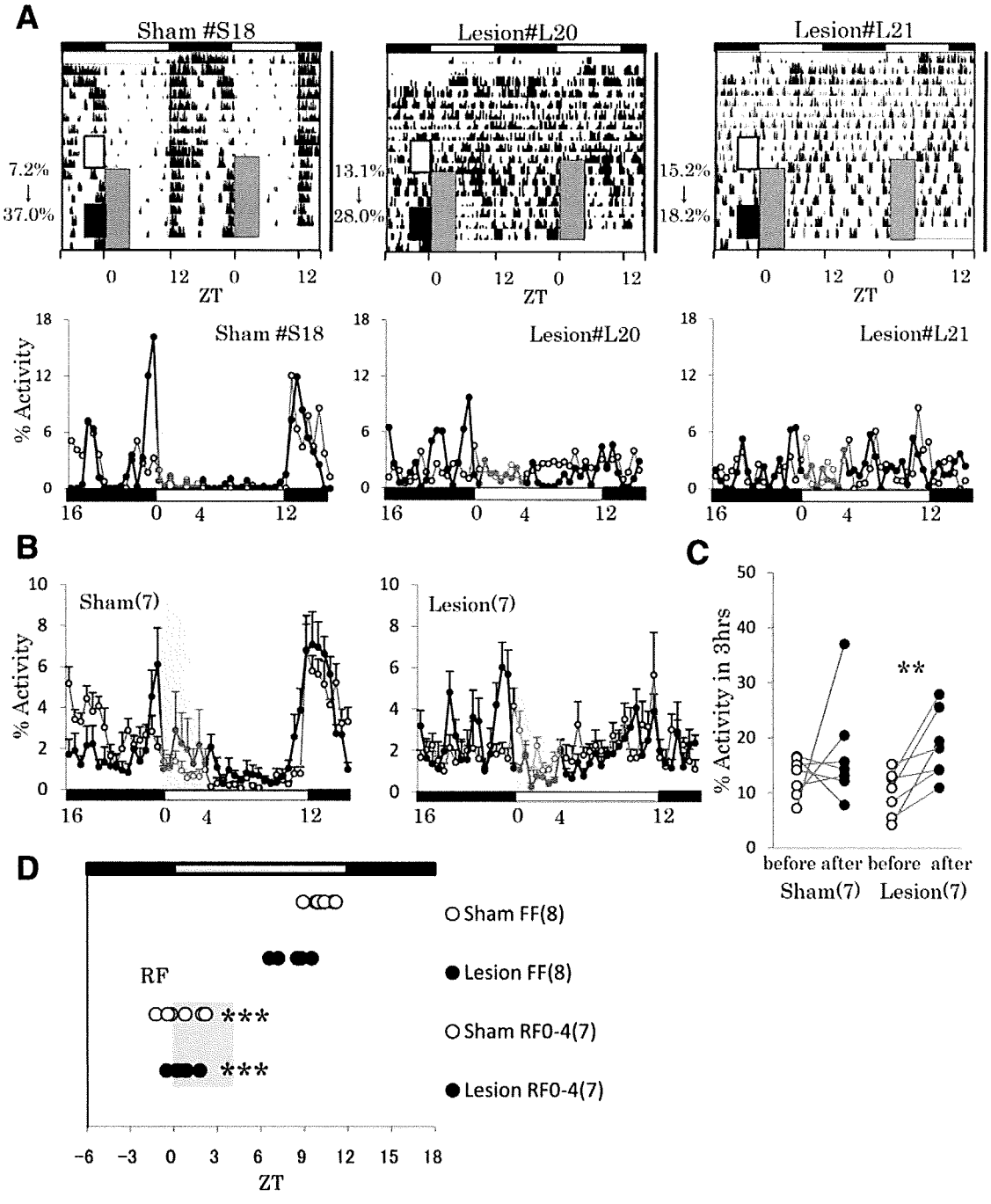

Figure 3. Effect of MBH lesions on restricted feeding (ZT0-ZT4)–induced food anticipatory activity rhythm and liver bioluminescence rhythms. (A) Examples of double-plotted actograms of sham-operated (#S18) or MBH-lesioned mice (#L20 and #L21) under a restricted feeding schedule. The axis bar in each graph indicates the day path after surgery. Horizontal open and closed bars indicate the light and dark periods, respectively. The restricted feeding time (gray rectangle box) was set at ZT0-ZT4 for 7 days after a 10-day surgery recovery period. Sham-operated mice (#S18) showed the strong anticipation (change of percentage activity from 7.2% before [white rectangle box] to 37.0% after [black rectangle box]). Two representative examples of lesioned mice are shown. Lesion #L21 shows almost no anticipation (change of percentage activity from 15.2% before [white rectangle box] to 18.2% after [black rectangle box]), but lesion #L20 shows moderate anticipation (change of percentage activity from 13.1% before [white rectangle box] to 28.0% after [black rectangle box]). In the lower panel of each example, the mean daily percentage activity before (open circle) and after (closed circle) restricted feeding (gray rectangle) is shown. (B) Percentage change of locomotor activity. Mean daily percentage activity of all mice before (open circle) and after (closed circle) restricted feeding (gray rectangle) is shown. (C) Percentage activity was calculated by the following formula: 100 × (activity counts [ZT21-ZT0, hatched rectangle box in Figure 3A] / daily 24-h activity counts) during the last 3 days before (open circle) or after (closed circle) the restricted feeding schedule. Each circle in the figure indicates each specific sample. $^{**}p < 0.01$ from before values (open circle); paired Student *t*-test. (D) Bioluminescence rhythm phase of *Per2*::luciferase mouse livers. Mice were sacrificed 8 days after a 7-day restricted feeding period (ZT0-ZT4). Data of sham-operated FF mice and MBH-lesioned FF mice were the same as in Figure 1D. Horizontal numbers indicate ZT. The rectangle area indicated by RF corresponds to the restricted feeding time in vivo. $^{***}p < 0.001$ from free-feeding mice; Fisher PLSD test.

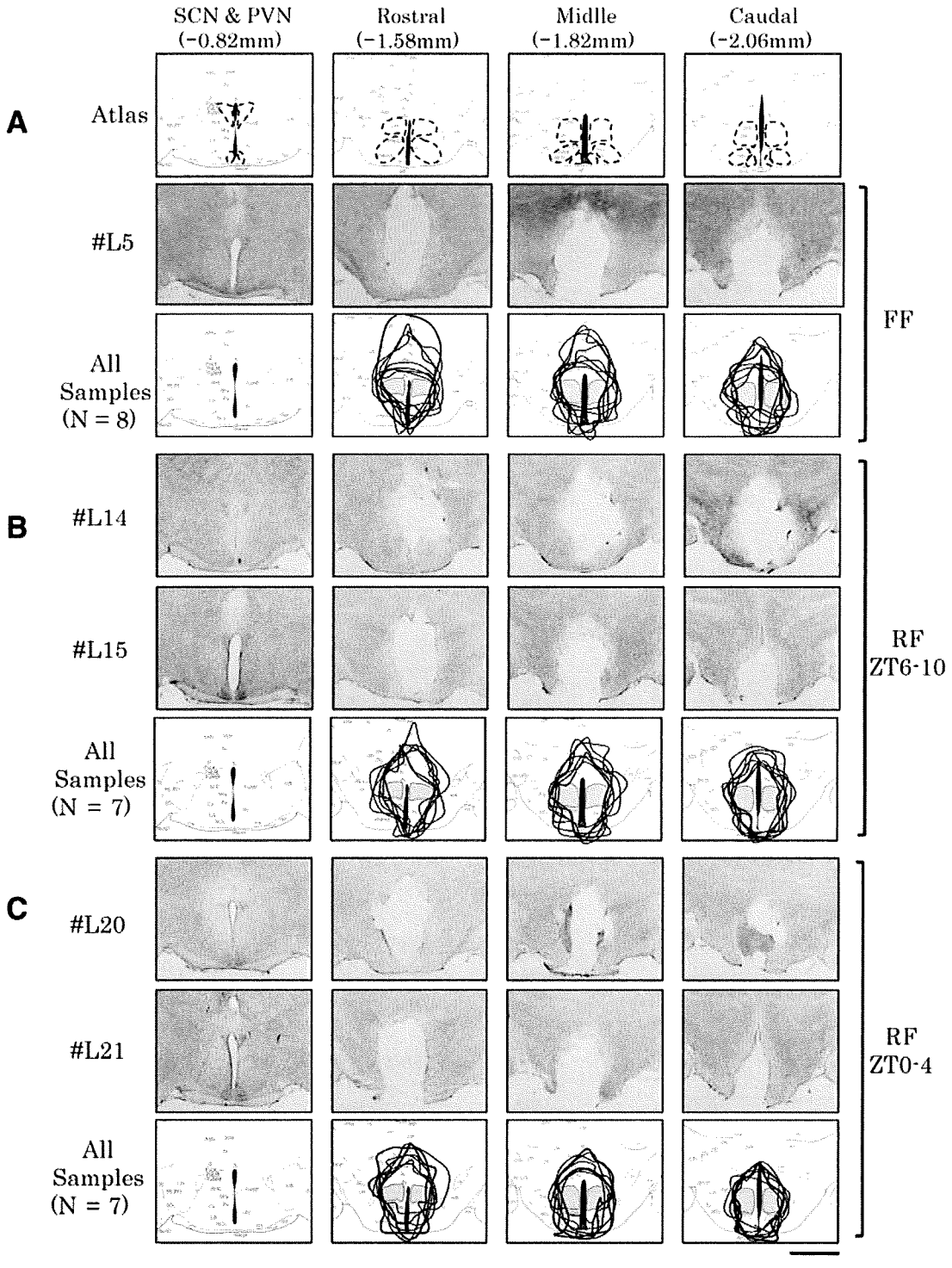

Figure 4. Representative photomicrographs of MBH lesion areas stained with cresyl violet and the size/region of the lesion areas. (A) Representative photomicrographs of MBH lesion areas staining with cresyl violet (#L5) and MBH lesion areas of this experiment ($N = 8$, for the MBH lesions). Dotted lines in the figure (upper panel) show the border of each SCN/PVN, DMH, VMH, and ARC by referencing a mouse brain atlas. Sample slices were from the suprachiasmatic nucleus (SCN)/paraventricular nucleus (PVN) and the rostral, middle, and caudal levels of the DMH in mouse #L5 (middle panel). In the lower panel, 8 circle lines at each level of the DMH show the border of the lesion area for all lesioned mice ($N = 8$). (B) Representative photomicrographs of MBH lesion areas staining with cresyl violet (sample #L14 and #L15). Sample slices were from the SCN/PVN and the rostral, middle, and caudal levels of the DMH. In the lower panel, 7 circle lines at each level of the DMH show the border of the lesion areas for all lesioned mice ($N = 7$). (C) Representative photomicrographs of MBH lesion areas staining with cresyl violet (sample #L20 and #L21). Sample slices were from the SCN/PVN and the rostral, middle, and caudal levels of the DMH. In the lower panel, 7 circle lines at each level of the DMH show the border of the lesion area for all lesioned mice ($N = 7$). Calibration bar indicates 1 mm.

FAA was clearly observed in sham-operated mice when restricted feeding was applied for ZT6-ZT10 because locomotor activity was low during ZT3-ZT6 of the free-feeding conditions. In contrast, it was difficult to see FAA when restricted feeding was applied for ZT0-ZT4 because locomotor activity was high during ZT21-ZT0 of the free-feeding conditions. The present results demonstrated that MBH destruction attenuated the FAA formation produced by restricted feeding during ZT6-ZT10. The increase in activity during the period of FAA (ZT3-ZT6) was 607% in sham-operated animals and 137% in the lesioned animals and resulted in a 73% reduction of the activity increase. Gooley et al. (2006) used a measurement similar to the above estimation and showed that the restricted feeding–induced increase in daytime behavior was reduced by 80.2% in DMH-lesioned rats. These results are remarkably consistent with the current study despite the use of a different species, lesioning method, and method for measuring FAA.

We made fairly large lesions that extended well beyond the DMH and included areas of the DMH, VMH, and ARC. We found that animals lost a very large component of their activity rhythms and had lower baseline activity levels, observations that reproduced the findings of Chou et al. (2003) and Gooley et al. (2006). Therefore, the lesioned mice used in the current study would be considered animals that had the physiological earmarks of complete DMH lesions. Conversely, it is possible that some of the effects we observed may have been due to the inclusion of adjacent cell groups. Previous studies that created lesions in the VMH and other adjacent areas as "control lesions" to eliminate such a possibility did not affect the entrainment of food. The current work lacks this control study. To conclude whether DMH lesions alone or MBH lesions (DMH lesions + surrounding nucleus lesions) are critical for FAA formation, future work will include the above described experimental group of control lesions.

Although some DMH-lesioned mice attenuated FAA formation (see #L15 in Figure 2 and #21 in Figure 3), these mice showed a clear advance of *Per2* rhythm by restricted feeding. Therefore, the present results indicate dissociations between behavioral FAA rhythms and those of peripheral clock gene expression. The findings are consistent with studies of Feillet et al. (2006), who demonstrated that *Per2* mutant mice exhibit very weak FAA rhythms but have a strong phase advance of peripheral clock gene expression. Taken together, these results indicate that restricted feeding–induced entrainment of peripheral clock genes occurs outside the DMH, in neuronal networks, and/or metabolically important peripheral tissue. In other words, we propose that feeding-related signals synchronize central and peripheral circadian clocks by parallel entrainment pathways.

The second important finding of this study is that MBH-lesioned animals had a loss of rhythmicity in locomotor activity but did not have a loss of rhythm of *Per2* expression in the liver. In addition, there was no dispersion of phase in liver tissues among MBH-lesioned mice. Activity rhythms in the MBH-lesioned mice were essentially absent when food was available *ad libitum*. If activity rhythms, and presumably feeding rhythms, are absent, the liver clocks will be desynchronized between mice and the phases of mice dispersed. To address this possibility, future studies will examine the feeding rhythm of MBH-lesioned, behavioral arrhythmic mice. Previously, it has been shown that SCN-lesioned mice exhibit arrhythmicity of behavioral rhythm and dispersed phase of liver rhythm (Yoo et al., 2004). In the present study, the SCN and PVN are intact and can convey the LD information from the SCN to the liver clock, so the phase of the liver clock in MBH-lesioned mice was not dispersed. It is known that the SCN conveys its "timing" signal to the periphery via 3 different routes: neural connections (autonomic branches), hormonal cues (corticosterone, melatonin, and growth hormone), and rhythmic feeding/activity behavior (Buijs and Kalsbeek, 2001; Guo et al., 2005).

The third important finding of this study is that we have found a 2-h phase advance of the bioluminescence rhythm peak in MBH-lesioned mice when compared to sham-operated mice. The weakened signals from the SCN to the liver clock in MBH-lesioned mice may be associated with phase advance of the liver clock. Many anatomical/physiological experiments have suggested that the liver receives a rich innervation of sympathetic and parasympathetic nerves from the PVN (Buijs and Kalsbeek, 2001). Liver glucocorticoids, adrenaline, and sympathetic nerve stimulation can either elicit a phase shift or trigger rhythmic gene expression (Balsalobre et al., 2000; Terazono et al., 2003). Destruction of adrenergic innervations by 6-hydroxy dopamine partially reduces *Per1* gene expression in the liver (Terazono et al., 2003), and a complete surgical hepatic sympathectomy causes a 4-h phase advance of the *Per2* and *Cry1* peaks without affecting the amplitude of gene expression (Cailotto et al., 2005). Therefore, a large hypothalamic lesion may reduce sympathetic activity in the liver and may result in a phase advance.

In summary, the mouse MBH consists of important brain regions responsible for the maintenance of

normal phase position of the liver clock and for restricted feeding–induced FAA rhythm. However, the MBH does not seem to be important for the restricted feeding–induced entrainment of the liver clock.

ACKNOWLEDGMENTS

This study was partially supported by grants awarded to S.S. from grants-in-aid for Scientific Research (20390065, 19659058) as well as from the Nakashima Foundation (2008) and Urakami Shokuhin Foundation (2008).

REFERENCES

Balsalobre A, Brown SA, Marcacci L, Tronche F, Kellendonk C, Reichardt HM, Schutz G, and Schibler U (2000) Resetting of circadian time in peripheral tissues by glucocorticoid signaling. Science 289:2344-2347.

Buijs RM and Kalsbeek A (2001) Hypothalamic integration of central and peripheral clocks. Nat Rev Neurosci 2:521-526.

Cailotto C, La Fleur SE, Van Heijningen C, Wortel J, Kalsbeek A, Feenstra M, Pévet P, and Buijs RM (2005) The suprachiasmatic nucleus controls the daily variation of plasma glucose via the autonomic output to the liver: are the clock genes involved? Eur J Neurosci 22:2531-2540.

Chou TC, Scammell TE, Gooley JJ, Gaus SE, Saper CB, and Lu J (2003) Critical role of dorsomedial hypothalamic nucleus in a wide range of behavioral circadian rhythms. J Neurosci 23:10691-10702.

Cone RD, Cowley MA, Butler AA, Fan W, Marks DL, and Low MJ (2001) The arcuate nucleus as a conduit for diverse signals relevant to energy homeostasis. Int J Obes Relat Metab Disord 5:S63-S67.

Damiola F, Le Minh N, Preitner N, Kornmann B, Fleury-Olela F, and Schibler U (2000) Restricted feeding uncouples circadian oscillators in peripheral tissues from the central pacemaker in the suprachiasmatic nucleus. Genes Dev 14:2950-2961.

Davidson AJ, Poole AS, Yamazaki S, and Menaker M (2003) Is the food-entrainable circadian oscillator in the digestive system? Genes Brain Behav 2:32-39.

Feillet CA, Ripperger JA, Magnone MC, Dulloo A, Albrecht U, and Challet E (2006) Lack of food anticipation in Per2 mutant mice. Curr Biol 16:2016-2022.

Gooley JJ, Schomer A, and Saper CB (2006) The dorsomedial hypothalamic nucleus is critical for the expression of food-entrainable circadian rhythms. Nat Neurosci 9:398-407.

Guo H, Brewer JM, Champhekar A, Harris RB, and Bittman EL (2005) Differential control of peripheral circadian rhythms by suprachiasmatic-dependent neural signals. Proc Natl Acad Sci U S A 102:3111-3116.

Hara R, Wan K, Wakamatsu H, Aida R, Moriya T, Akiyama M, and Shibata S (2001) Restricted feeding entrains liver clock without participation of the suprachiasmatic nucleus. Genes Cells 6:269-278.

Hayasaka N, Yaita T, Kuwaki T, Honma S, Honma K, Kudo T, and Shibata S (2007) Optimization of dosing schedule of daily inhalant dexamethasone to minimize phase shifting of clock gene expression rhythm in the lungs of the asthma mouse model. Endocrinology 148:3316-3326.

Landry GJ, Simon MM, Webb IC, and Mistlberger RE (2006) Persistence of a behavioral food-anticipatory circadian rhythm following dorsomedial hypothalamic ablation in rats. Am J Physiol Regul Integr Comp Physiol 290:R1527-R1534.

Landry GJ, Yamakawa GR, Webb IC, Mear RJ, and Mistlberger RE (2007) The dorsomedial hypothalamic nucleus is not necessary for the expression of circadian food-anticipatory activity in rats. J Biol Rhythms 22:467-478.

Moriya T, Aida R, Kudo T, Akiyama M, Doi M, Hayasaka N, Nakahata N, Okamura H, and Shibata S (2009) The dorsomedial hypothalamic nucleus is not necessary for food-anticipatory circadian rhythms of behavior, temperature or clock gene expression in mice. Eur J Neurosci 29:1447-1460.

Ohta H, Xu S, Moriya T, Iigo M, Watanabe T, Nakahata N, Chisaka H, Hanita T, Matsuda T, Ohura T, et al. (2008) Maternal feeding controls fetal biological clock. PLoS ONE 3:e2601.

Poulin AM and Timofeeva E (2008) The dynamics of neuronal activation during food anticipation and feeding in the brain of food-entrained rats. Brain Res 1227:128-141.

Ribeiro AC, Sawa E, Carren-LeSauter I, LeSauter J, Silver R, and Pfaff DW (2007) Two forces for arousal: pitting hunger versus circadian influences and identifying neurons responsible for changes in behavioral arousal. Proc Natl Acad Sci U S A 104:20078-20083.

Rodgers RJ, Ishii Y, Halford JC, and Blundell JE (2002) Orexins and appetite regulation. Neuropeptides 36: 303-325.

Saper CB, Lu J, Chou TC, and Gooley J (2005a) The hypothalamic integrator for circadian rhythms. Trends Neurosci 28:152-157.

Saper CB, Scammell TE, and Lu J (2005b) Hypothalamic regulation of sleep and circadian rhythms. Nature 437:1257-1263.

Stokkan KA, Yamazaki S, Tei H, Sakaki Y, and Menaker M (2001) Entrainment of the circadian clock in the liver by feeding. Science 291:490-493.

Terazono H, Mutoh T, Yamaguchi S, Kobayashi M, Akiyama M, Udo R, Ohdo S, Okamura H, and Shibata S (2003) Adrenergic regulation of clock gene expression in mouse liver. Proc Natl Acad Sci U S A 100:6795-6800.

Wakamatsu H, Yoshinobu Y, Aida R, Moriya T, Akiyama M, and Shibata S (2001) Restricted-feeding-induced anticipatory activity rhythm is associated with a phase-shift of the expression of mPer1 and mPer2 mRNA in the cerebral cortex and hippocampus but not in the suprachiasmatic nucleus of mice. Eur J Neurosci 13:1190-1196.

Yoo SH, Yamazaki S, Lowrey PL, Shimomura K, Ko CH, Buhr ED, Siepka SM, Hong HK, Oh WJ, Yoo OJ, et al. (2004) PERIOD2::LUCIFERASE real-time reporting of circadian dynamics reveals persistent circadian oscillations in mouse peripheral tissues. Proc Natl Acad Sci USA 101:5339-5346.

EJN fens EUROPEAN JOURNAL OF NEUROSCIENCE

European Journal of Neuroscience, Vol. 29, pp. 1447–1460, 2009 doi:10.1111/j.1460-9568.2009.06697.x

BEHAVIORAL NEUROSCIENCE

The dorsomedial hypothalamic nucleus is not necessary for food-anticipatory circadian rhythms of behavior, temperature or clock gene expression in mice

Takahiro Moriya,[1,2] Reiko Aida,[1] Takashi Kudo,[3] Masashi Akiyama,[1] Masao Doi,[4,5] Naomi Hayasaka,[4] Norimichi Nakahata,[2] Ralph Mistlberger,[6] Hitoshi Okamura[4,5] and Shigenobu Shibata[1,3]

[1]Department of Pharmacology and Brain Science, School of Human Sciences, Waseda University, Tokorozawa, Saitama, 359-1192, Japan

[2]Department of Cellular Signaling, Graduate School of Pharmaceutical Sciences, Tohoku University, Sendai 980-8578, Japan

[3]Department of Pharmacology, School of Science and Engineering, Waseda University, Tokyo, 169-0072, Japan

[4]Division of Molecular Brain Science, Department of Brain Sciences, Kobe University Graduate School of Medicine, Kobe, 650-0017, Japan

[5]Department of Systems Biology, Graduate School of Pharmaceutical Sciences, Kyoto University, Kyoto, 606-8501, Japan

[6]Department of Psychology, Simon Fraser University, Burnaby BC Canada V5A 1S6

Keywords: arcuate nucleus, food entrainment, *mBMAL1*, *Period* genes, suprachiasmatic nucleus

Abstract

Circadian rhythms in mammals are regulated by a light-entrainable circadian pacemaker in the hypothalamic suprachiasmatic nucleus and food-entrainable oscillators located elsewhere in the brain and body. The dorsomedial hypothalamic nucleus (DMH) has been proposed to be the site of oscillators driving food-anticipatory circadian rhythms, but this is controversial. To further evaluate this hypothesis, we measured clock gene, temperature and activity rhythms in intact and DMH-ablated mice. A single 4-h midday feeding after an overnight fast induced *mPer1* and *mPer2* mRNA expression in the DMH, arcuate nucleus, nucleus of the solitary tract and area postrema, and reset daily rhythms of *mPer1*, *mPer2* and *mBMAL1* in the DMH, arcuate and neocortex. These rhythms persisted during 2 days of food deprivation after 12 days of scheduled daytime feeding. Acute induction of DMH *mPer1* and *mPer2* was *N*-methyl-D-aspartate (NMDA) receptor-dependent, whereas rhythmic expression after 6 days of restricted feeding was not. Thermal DMH lesions did not affect acute induction or rhythmic expression of clock genes in other brain regions in response to scheduled daytime feeding. DMH lesions attenuated mean daily activity levels and nocturnality but did not affect food-anticipatory rhythms of activity and body temperature in either light–dark or constant darkness. These results confirm that the DMH and other brain regions express circadian clock gene rhythms sensitive to daytime feeding schedules, but do not support the hypothesis that DMH oscillations drive food-anticipatory behavioral or temperature rhythms.

Introduction

The discovery of the suprachiasmatic nucleus (SCN) as the site of a master pacemaker necessary for generating circadian rhythms of behavior and physiology, and for synchronizing these to daily light–dark (LD) cycles, is a modern success story in localization of function within the mammalian brain (Weaver, 1998). It is now recognized that other brain regions and peripheral organs and tissues also contain circadian oscillators, and that for many of these it is food and not light that is the dominant stimulus controlling circadian phase. Thus, if nocturnal rodents are forced or enticed to eat primarily during the middle of the light period, when they would normally be sleeping, circadian rhythms of clock gene expression (e.g. *Per1*, *Per2*, *Cry1*, *Cry2*, *BMAL1*) and cellular functions in most organs and many brain regions phase shift to align with mealtime (Boulos & Terman, 1980; Damiola *et al.*, 2000; Stokkan *et al.*, 2001; Wakamatsu *et al.*, 2001; Abe *et al.*, 2002; Guilding & Piggins, 2007; Angeles-Castellanos *et al.*, 2007; Angeles-Castellanos *et al.*, 2008; Verwey *et al.*, 2007; Waddington Lamont *et al.*, 2007; Feillet *et al.*, 2008). A behavioral rhythm of food-anticipatory activity also emerges, in the form of increased wheel running, food-bin approaches or general activity beginning several hours prior to mealtime, in parallel with increased body temperature and release of metabolic hormones (Mistlberger, 1994; Escobar *et al.*, 1998; Diaz-Munoz *et al.*, 2000; Morgado *et al.*, 2008). Notably, food-anticipatory rhythms persist following complete SCN ablation (Stephan *et al.*, 1979; Hara *et al.*, 2001), indicating control by entrainable oscillators located elsewhere (Mistlberger, 1994; Stephan, 2002).

Correspondence: Dr S. Shibata, [3]Department of Pharmacology, as above.
E-mail: shibatas@waseda.jp

Received 30 September 2008, revised 3 February 2009, accepted 6 February 2009